



Norwegian
Meteorological Institute
met.no



met.no report

no. 3/2008
Remote Sensing

QuikScat Validation Report

Birgitte R. Furevik, Lars-Anders Breivik and Frank Tvetter

Title QuikSCAT validation report	Date 22.02.2008
Section Forecasting Division for Western Norway	Report no. 3/2008 Remote Sensing
Author(s) Birgitte R. Furevik, Lars-Anders Breivik and Frank Tveter	Classification <input checked="" type="checkbox"/> Free <input type="checkbox"/> Restricted
	ISSN 1503-8025
	e-ISSN
Client(s) STATOILHYDRO ASA	Client's reference
Abstract QuikScat winds are validated against observations from Weather Station M, platforms and buoys on the Norwegian shelf and against synoptic stations on Hopen and Bjørnøya. The QuikScat winds compare very well to offshore observations with correlations of 0.89-0.93. Significantly poorer correlation with the two land based stations can be explained by topographic effects, distance between the compared locations and possible ice contaminations during some periods. The high quality of scatterometer winds and the spatial coverage makes these data very well suited for validation of e.g. surface wind from atmosphere models.	
Keywords QuikScat, SeaWinds, scatterometer, remote sensing, validation, wind	

Disciplinary signature	Responsible signature
 _____	 _____

1 Background

The objective of this work is to validate the QuikScat winds against *in situ* observations over the whole range of wind speeds. Validation of QuikScat data against research vessels and buoys give accuracies of 1.2-1.7m/s and 14-15° in root-mean-square difference (Bourassa et al., 2003; Chelton and Freilich, 2005). A validation of QuikScat data in high latitude oceans around Norway has not earlier been performed.

The scatterometer is a radar instrument emitting microwave pulses toward the sea surface and measuring the backscattered signal. The backscatter is depending on the small capillary/gravity sea waves. These waves in turn depend on the near surface wind. An empirical relationship are found between the backscatter measurements and the 10m wind speed and wind direction relative the antenna viewing angle. From a polar orbiting satellite the scatterometer instrument cover large ocean areas and provides very useful wind information for operational meteorology.

In 1991 the ERS-1 satellite was launched. It was equipped with a scatterometer with three antennas giving three look angles. The follower instrument on ERS-2 launched in 1995 still provides high quality wind observations. From the start the ERS-1 and -2 data has been evaluated and utilized at met.no (Breivik and Haugse, 1994). Since 1993 the ERS scatterometer data were assimilated in the operational numerical weather prediction model (Breivik, 1993; Schyberg and Breivik, 2002). In 2001 met.no started work on utilizing SeaWinds scatterometer data from the NOAA/NESDIS satellite QuikSCAT (Tvetter 2002 and 2006). The SeaWinds instrument differs from the ERS scatterometer in that it is one antenna varying the viewing angles by rotating (Pencil-beam). This gives large surface coverage, but in some cases increases the ambiguity problem by introducing more than two likely solutions. In addition SeaWinds operate in a higher microwave frequency (Ku-band), which makes the returned signals more sensitive to rain contamination compared to the ERS (C-band). For additional information on QuikSCAT, see <http://winds.jpl.nasa.gov/missions/quikscat/>.

In October 2006 the operational meteorological satellite METOP was launched. It flies a follower scatterometer from ERS, the ASCAT instrument. With three satellites in the METOP series ASCAT is planned to provide data until 2020. Given the long time series of scatterometer data now available the data is well suited for time series and studies of regional as well as global ocean wind climate.

Wind direction ambiguity

Depending on the antenna geometry, it turns out that several possible surface winds can explain the observed backscatter. For instance an ERS backscatter measurement is usually converted into two wind vector ambiguities, with almost the same wind speed but pointing in opposite directions (180 deg ambiguity). In more technical terms we can say that the wind vector ambiguities represent the mean value of each of the Normal components in the probability density function for the true wind given the backscatter measurements. For QuikSCAT, four ambiguities are used to describe the probability density function for the true wind vector given the backscatter measurements. Each of these ambiguities has an a-priori probability (or a weight used when the Normal components are added together). The ambiguity with highest a-priori probability is said to be the 'rank 1 ambiguity', the ambiguity with the second highest a-priori probability is said to have rank 2 etc. A main challenge exploiting scatterometer data is therefore the ambiguity removal i.e. choosing the right solution. To do this a first guess wind field from a numerical weather prediction (NWP) is used along with assumptions on consistency in the surface wind field (QuikScat User's Manual, 2006).

Equivalent Neutral Wind

The relation between radar backscatter and 10m wind is empirical and assuming that the atmosphere is neutrally stratified. The wind measured by scatterometer can thus be referred to as "Equivalent neutral wind" (Liu and Tang, 1996). Neutral condition is the most common situation over the open ocean, but exceptions occur over large areas e.g. for cold air outbreaks. The equivalent neutral wind is

higher than the actual wind for unstable conditions and lower under stable conditions. The largest corrections are needed for low wind speed values (<6m/s).

Rain contamination

The QuikSCAT measurements are sensitive to heavy rainfall. Heavy precipitation increases the radar backscatter and results in an overestimate of the wind speed. Experience from operational use at met.no indicates that around 10% of the received QuikSCAT measurements are rain contaminated resulting in around 2-4 m/s overestimate of wind speed. The wind direction estimate has not been observed to be affected. Other studies indicate that storms, rain and ambiguity selection errors are correlated (Draper and Long, 2002). However, the problem of rain contamination is most dominant in convective precipitation and much less in frontal precipitation. As a consequence the problem is larger at low latitudes and relatively small at high latitudes as the study area focused in this report.

Sea Ice

Sea ice can be a problem but ice infested areas are removed from the dataset. QuikSCAT is designed to measure ocean surface wind. However it can also be used to derive sea ice information. Backscattering is relatively isotropic over sea ice compared to the strong anisotropic behaviour over open water which is utilized for wind direction detection. Over sea ice backscatter is also dependent on ice age, and QuikSCAT data are used both for ice edge and ice type as well as ice drift detection. For more information and examples see e.g. <http://www.seaice.dk/test.N/> and under “Other Sea Ice products” at <http://mersea.met.no/docs/> .

The data used in the validation are summarised in Section 2 and the methodology is described in Section 3. Section 4 presents the analysis of the collocated data at the seven locations including the statistics as described above. Discussion of the results, possible sources of error of the various data and recommendations are given in section 5. QuikScat error sources have also been discussed above. Plots of the collocated time series of wind speed and wind direction from QuikScat and *in situ* at the seven sites are shown in the appendix.

2 Observations

Observations from seven locations have been used (Table 1). For the land based stations it is necessary to choose a point well offshore for extracting QuikScat data, since the presence of land can cause scatter in the QuikScat observations due to fewer data points and erroneous values (Furevik et al., 2006). A map of Hopen and Bjørnøya with the location of the measurement point, location of the QuikScat point and the topography is shown in Figure 1. QuikScat is a polar orbiting satellite and therefore covers the northern regions (such as the Barents Sea) more frequently than regions further south. The number of QuikScat observations per day is 2-7.

Table 1: Overview of the in situ observations used for verification of the QuikScat data.

Name	Latitude	Longitude	Qscat latitude	Qscat longitude	Period. Sampling. Height above sea level
Weather Station M	66N	2E	66N	2E	19.07.1999 – 31.12.2007. Hourly data. 15m
Buoy west	73.5N	15.5E	73.5N	15.5E	08.03.2007 – 31.12.2007. Hourly data. 3.5m
Buoy east	74N	30E	74N	30E	08.03.2007 – 25.12.2007. Hourly data. 3.5m
Bjørnøya	74.5167N	19.0167E	74.95N	19.0E	19.07.1999 – 31.12.2007. Hourly data. 16m
Hopen	76.5	25.0667	76.25N	25.5E	19.07.1999 – 31.12.2007. 3-hourly data. 6m
Gullfaks-C	61.2042N	2.2687E	61.2042N	2.2687E	19.07.1999 – 31.12.2007. 10min data. 143m*
Ekofisk	56.5N	3.2E	56.5N	3.2E	19.07.1999 – 31.12.2007. 10min data. 116m*

*Wind speed reduced to 10m above sea level has been used.

3 Method

The SeaWinds on QuikScat Level 2B product on 25km swath grid from July 1999 to January 2008 were downloaded from <http://podaac.jpl.nasa.gov/>. QuikScat data points within a radius of 25km of an *in situ* data location (i.e. the Qscat latitudes and longitudes given in Table 1) were extracted from the global data set. The standard ambiguity selection data set has been used, and all points where wind speed was retrieved were used for the collocation. The vector data (east and north components of the wind speeds) were spatially interpolated to the *in situ* location using a Gaussian distribution weighting function. The *in situ* winds were then interpolated in time to the QuikScat passage times (2-7 per day).

The correlation, ranging between -1 and 1, of QuikScat data (Y_i) with *in situ* data (X_i) is defined as

$$r = \frac{\sum_{i=1}^n (X_i - \bar{X})(Y_i - \bar{Y})}{\sqrt{[\sum_{i=1}^n (X_i - \bar{X})^2][\sum_{i=1}^n (Y_i - \bar{Y})^2]}}$$

where \bar{X} and \bar{Y} are the mean values of each data set and n is the number of measurements. The mean bias gives an estimate of the long term deviation of the two data sets

$$bias = \frac{\sum_{i=1}^n X_i - Y_i}{n}$$

and the root-mean-square deviation (*rmsd*) gives an estimate of the magnitude of the deviations

$$rmsd = \sqrt{\frac{\sum_{i=1}^n (X_i - Y_i)^2}{n}}$$

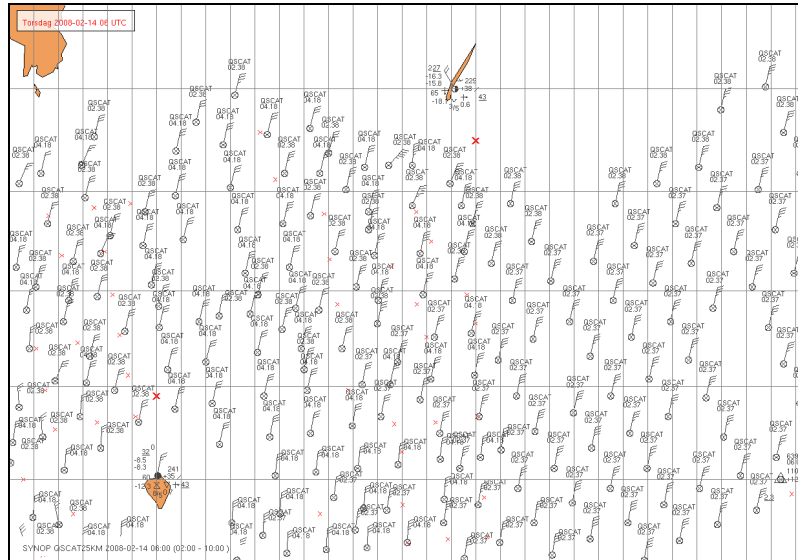


Figure 1: Map showing Bjørnøya and Hopen with the synoptic stations and an overlaid QuikScat wind field from February 14, 2008. The two red crosses are the locations to which QuikScat winds have been interpolated for comparison with the land stations.

4 Results

Based on the collocated data set for each of the seven locations presented as time series in the appendix, statistical parameters and comparison plots are produced. In Figure 2 - Figure 5 the scatter plots for wind speed and direction are shown. Due to the large number of data points the data are also plotted in quantile-quantile (Q-Q) plots to be able to investigate the distributions of the data sets.

The correlation in wind speed lies around 0.9 for the offshore stations (platforms, buoys and station M) while it is much lower for the land based stations (0.61 and 0.79). Ice may be present around Hopen and Bjørnøya in winter. Normally values containing ice are removed from the QuikScat data set, but in some periods we suspect contamination from ice, such as e.g. in January and February 2004 at Hopen (see appendix) where wind speeds are significantly higher than the *in situ* observations.

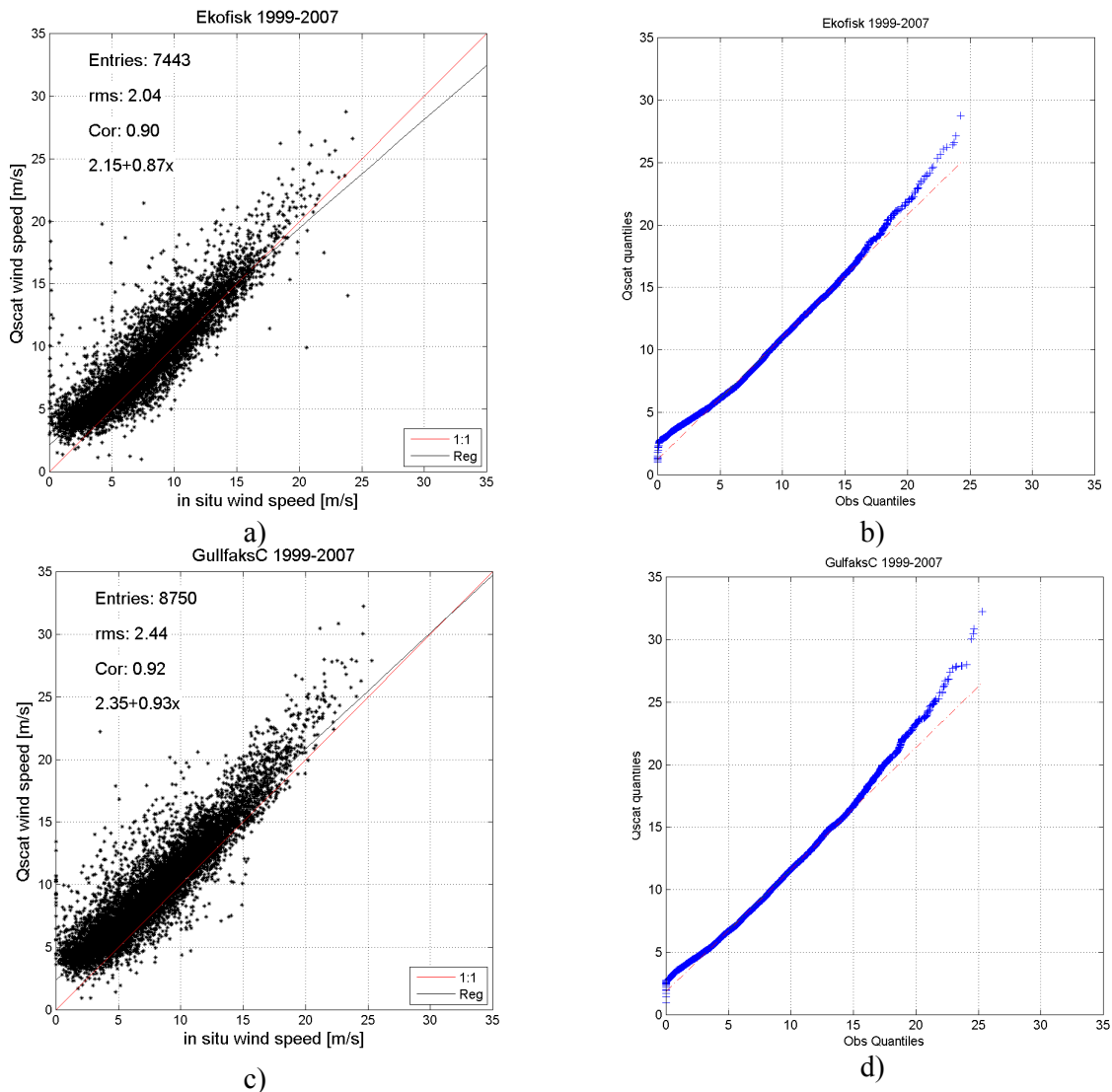


Figure 2: Scatter plots (left) and QQ plots (right) of QuikScat wind speed against in situ observations from Ekofisk (a-b) and Gullfaks C (c-d) offshore platforms. The linear regression line is plotted for each case (black line) and the correlation and root-mean-square deviation of QuikScat relative to *in situ* (rms) is given.

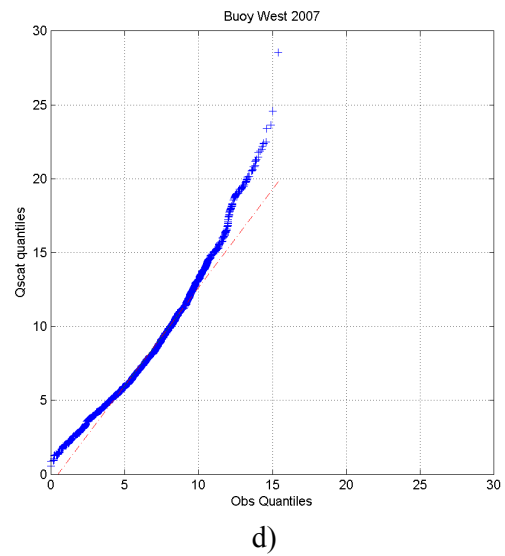
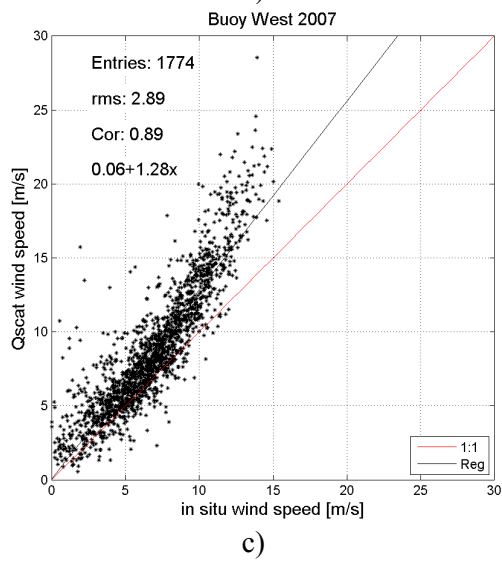
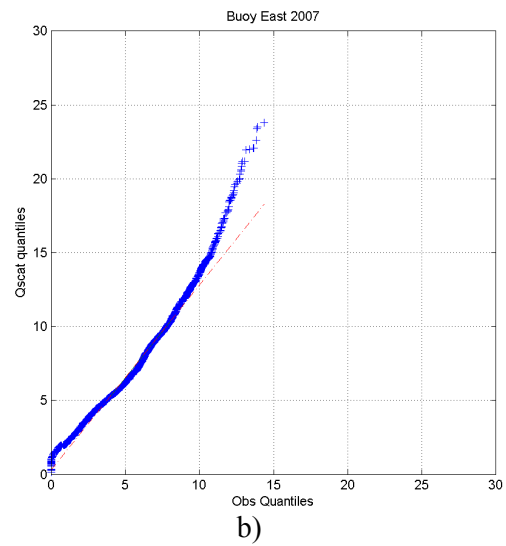
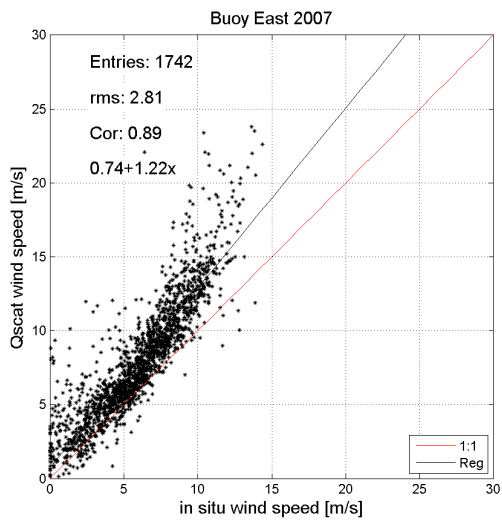
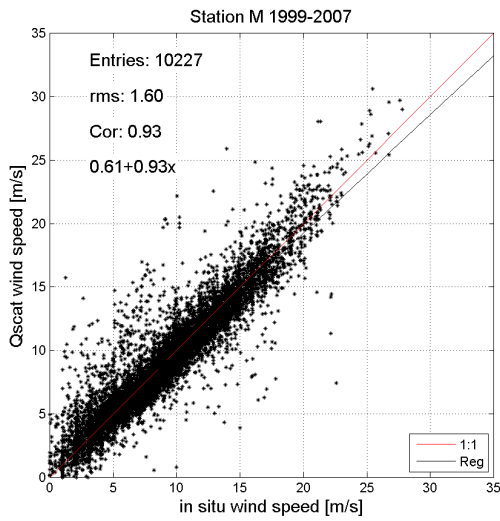
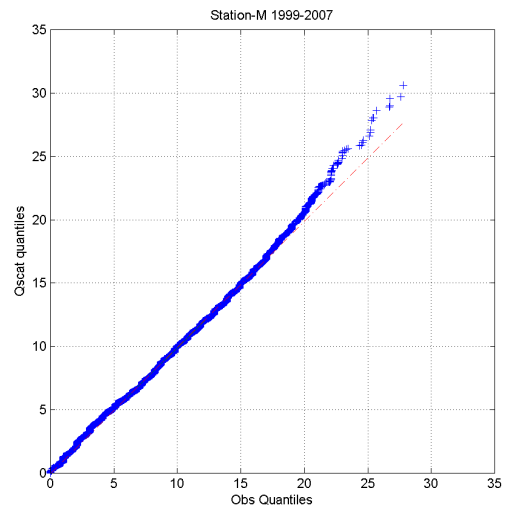


Figure 3: Scatter plots (left) and QQ plots (right) of QuikScat wind speed against in situ observations from the two buoys in the Barents Sea, denoted Buoy East and Buoy West. The linear regression line is plotted for each case (black line) and the correlation and root-mean-square deviation of QuikScat relative to *in situ* (rms) is given.



a)



b)

Figure 4: Scatter plots (left) and QQ plots (right) of QuikScat wind speed against in situ observations from weather station M. The linear regression line is plotted for each case (black line) and the correlation and root-mean-square deviation of QuikScat relative to *in situ* (rms) is given.

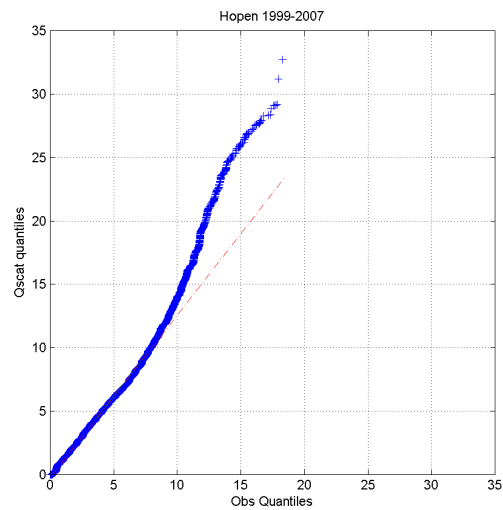
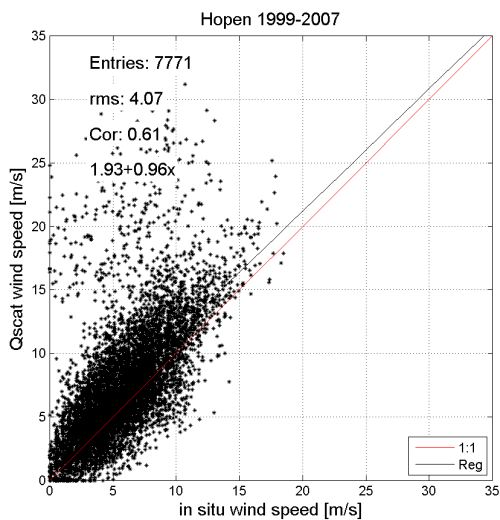
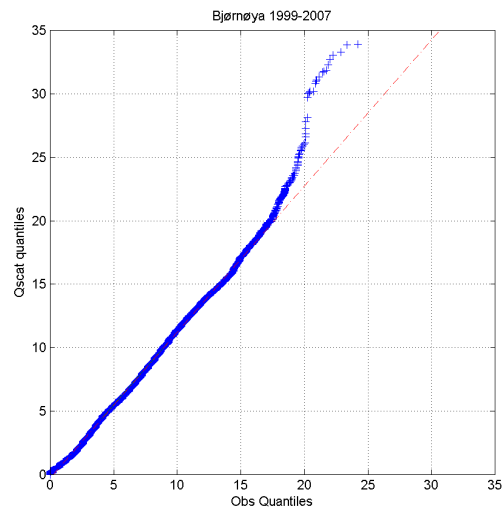
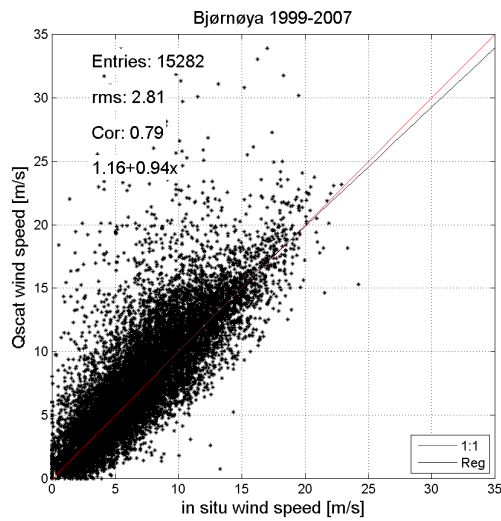


Figure 5: Scatter plots (left) and QQ plots (right) of QuikScat wind speed against in situ observations from Bjørnøya (a-b) and Hopen (c-d). QuikScat data were obtained from a location ~25km offshore. The linear regression line is plotted for each case (black line) and the correlation and root-mean-square deviation of QuikScat relative to *in situ* (rms) is given.

The wind direction and wind speed distribution is further illustrated by wind roses. Figure 6 – Figure 9 displays two wind roses per location, one for *in situ* (left) and one for QuikScat observations (right). The direction is presented as “coming from” (meteorological convention). The distance from the centre of the wind rose shows the percentage of occurrence.

Similar wind patterns from QuikScat and *in situ* are observed on most sites. The directional preferences in the platform observations may be due to sheltering effects on the wind sensor for certain wind directions and enhancement on others. From the scatter plots of wind direction (not shown) it is evident that in particular the Gullfaks-C sensor has had some systematic directional errors. Because of these errors, most directional data from 2006 on Gullfaks-C was removed when calculating the rms deviation. Relatively large differences are found for the land based stations, but the overall pattern is north-north easterly in both datasets. A good directional agreement is found with the buoys and weather station M.

Table 2 – Table 8 summarise the wind speed statistics (mean, median, mean bias, correlation, root-mean-square deviation (*rmsd*) of wind speed and direction, 90th and 95th percentile (P90 and P95) for each site. There is a clear difference in the results when comparing QuikScat with offshore and land based stations, the latter not suitable to represent the ocean wind conditions measured in a coarse satellite grid.

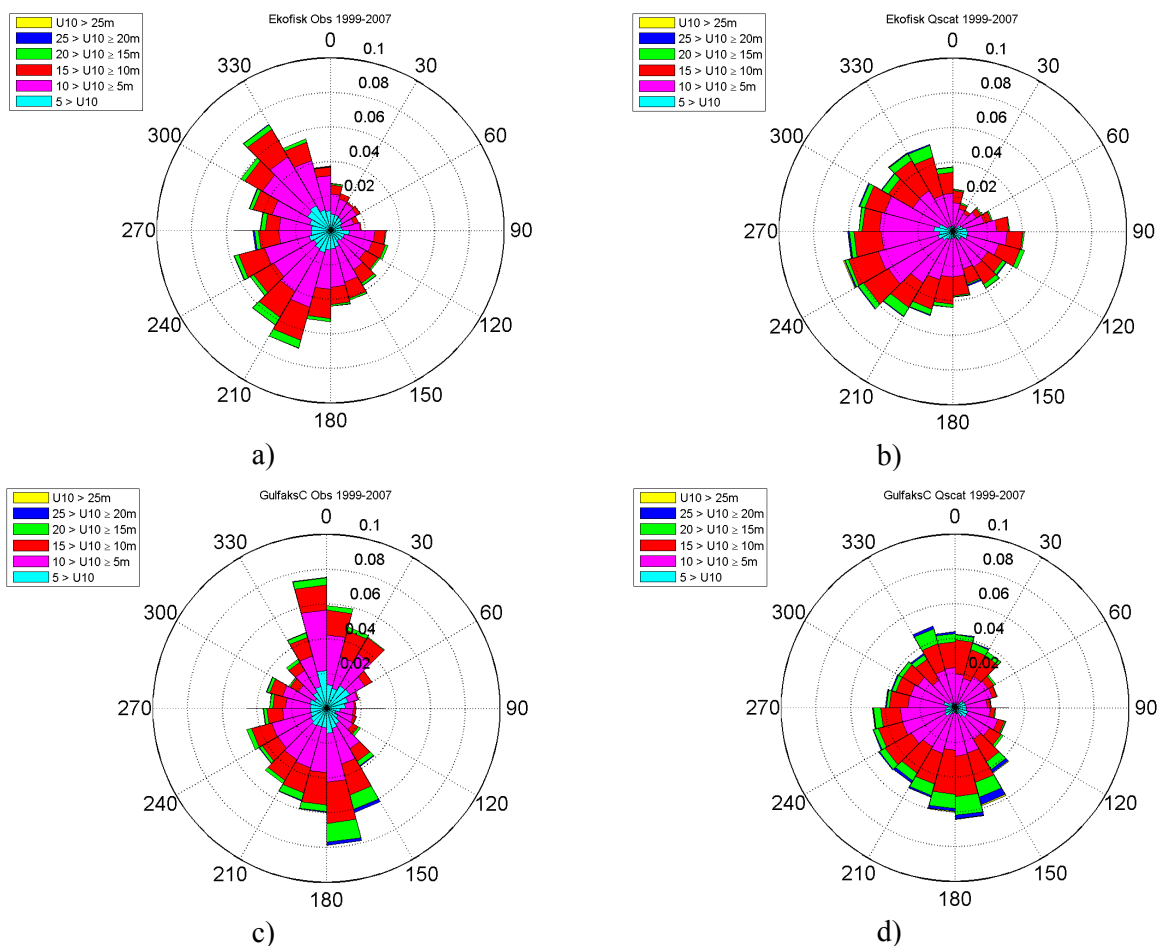


Figure 6: Wind roses for *in situ* observations (left) and QuikScat data (right) during the 8.5 year period at Ekofisk (a-b) and Gullfaks-C (c-d). The distance from the centre is given in percentage/100, wind direction is “coming from”.

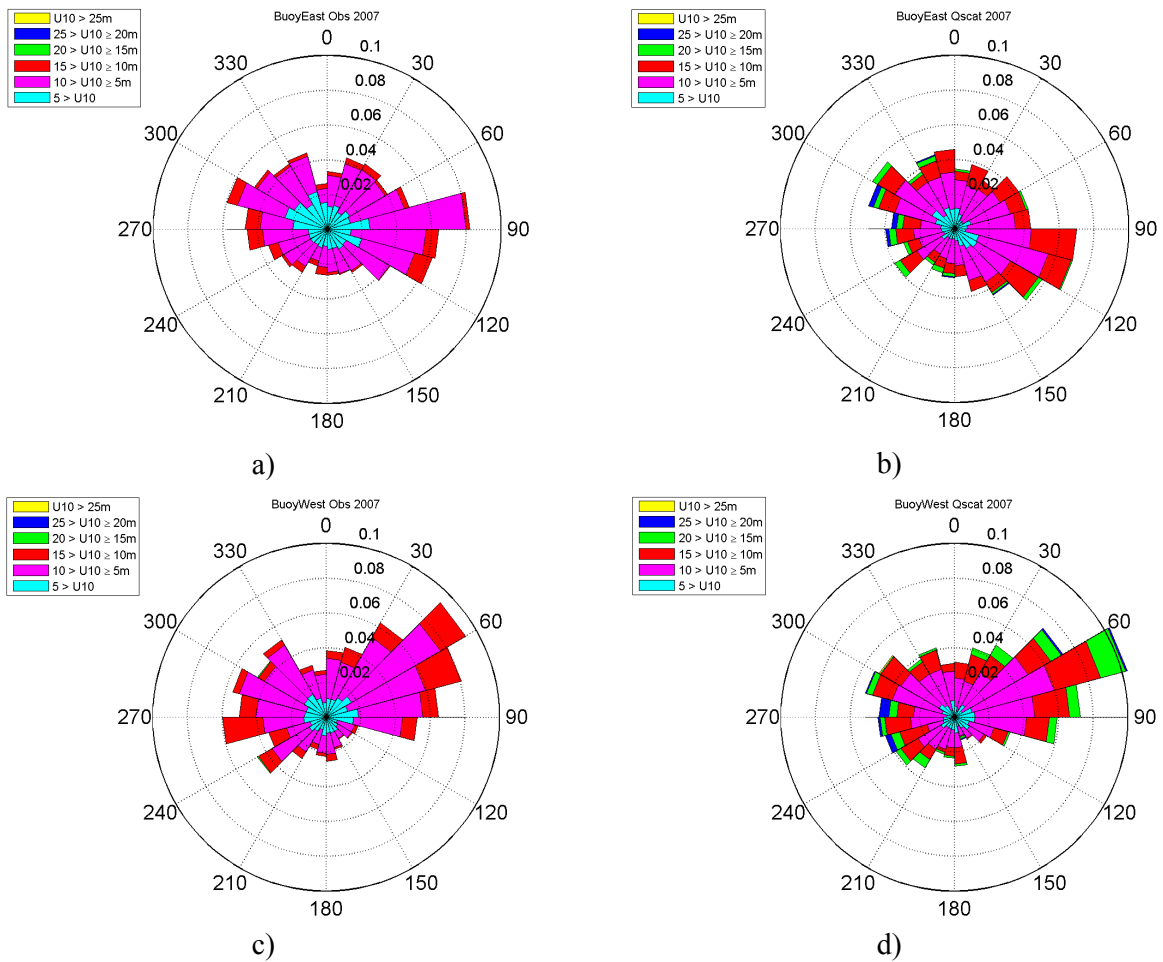


Figure 7: Wind roses for in situ observations (left) and QuikScat data (right) during the 9-month period for the eastern (a-b) and and western buoy location (c-d). The distance from the centre is given in percentage/100, wind direction is “coming from”.

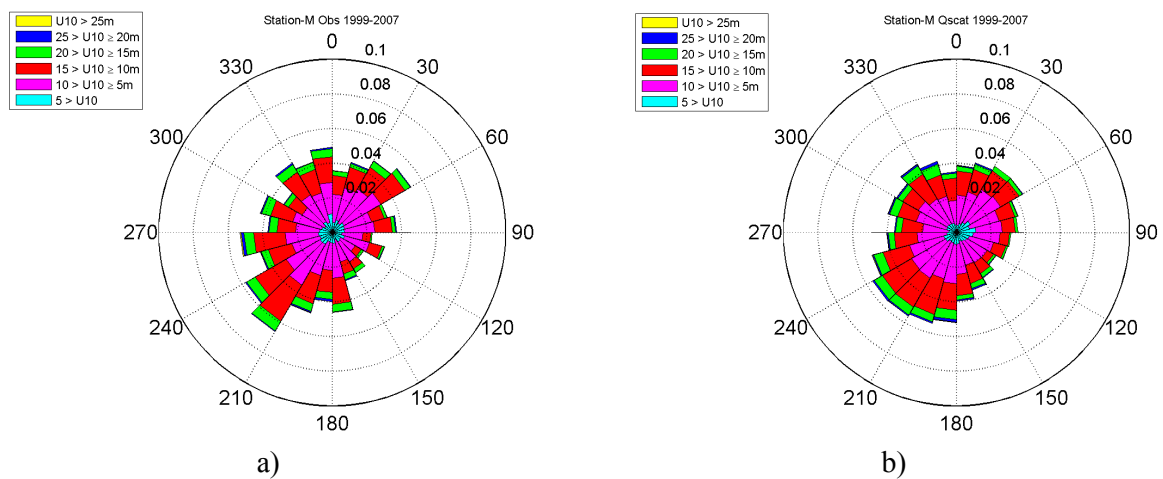


Figure 8: Wind roses for in situ observations (a) and QuikScat data (b) for Weather Station “M” during 8.5 years. The circles are given in percentage/100, wind direction is “coming from”.

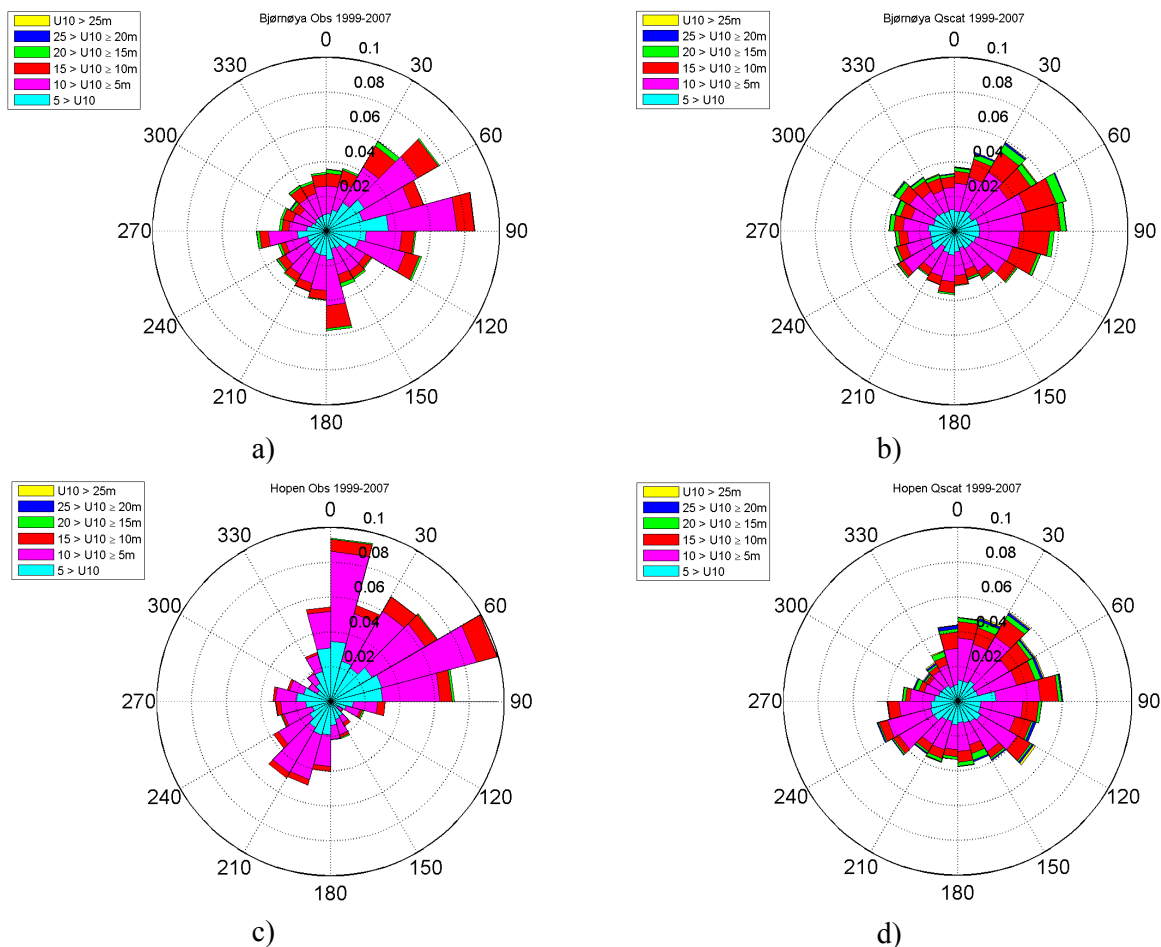


Figure 9: Wind roses for in situ observations (left) and QuikScat data (right) during 8.5 years for Bjørnøya (a-b) and Hopen (c-d). QuikScat observation point was taken offshore (~25km) from land. The distance from the centre is given in percentage/100, wind direction is “coming from”.

Table 2: Data statistics for QuikScat and observations at Ekofisk.

Data	Mean [m/s]	Median [m/s]	Bias [m/s]	Corr.	Rmsd		P90 [m/s]	P95 [m/s]
					Speed	Direction		
<i>In situ</i>	7.81	7.46	-	-	-	-	13.00	14.64
Satellite	8.91	8.27	1.10	0.90	2.04 m/s	29°	13.98	15.65

Table 3: Data statistics for QuikScat and observations at Gullfaks C.

Data	Mean [m/s]	Median [m/s]	Bias [m/s]	Corr.	Rmsd		P90 [m/s]	P95 [m/s]
					Speed	Direction		
<i>In situ</i>	8.00	7.52	-	-	-	-	13.72	15.73
Satellite	9.75	9.03	1.76	0.92	2.44 m/s	35°*	15.39	17.71

*Directional data from the period 15.03.2006-31.01.2007 were removed due to erroneous *in situ* directions.

Table 4: Data statistics for QuikScat and observations from Barents Sea Buoy East.

Data	Mean [m/s]	Median [m/s]	Bias [m/s]	Corr.	Rmsd		P90 [m/s]	P95 [m/s]
					Speed	Direction		
<i>In situ</i>	6.02	6.07	-	-	-	-	9.72	10.64
Satellite	8.06	7.60	2.45	0.89	2.81 m/s	35°	13.16	14.73

Table 5: Data statistics for QuikScat and observations from Barents Sea Buoy West.

Data	Mean	Median	Bias	Corr.	<i>Rmsd</i>		P90	P95
	[m/s]	[m/s]	[m/s]		Speed	Direction	[m/s]	[m/s]
<i>In situ</i>	6.59	6.63	-	-	-	-	10.74	11.98
Satellite	8.84	8.10	2.25	0.89	2.89 m/s	35°*	14.78	17.03

*Removed repetitions of 90° in *in situ* data.

Table 6: Data statistics for QuikScat and observations from Weather Station M.

Data	Mean	Median	Bias	Corr.	<i>Rmsd</i>		P90	P95
	[m/s]	[m/s]	[m/s]		Speed	Direction	[m/s]	[m/s]
<i>In situ</i>	9.24	8.75	-	-	-	-	15.00	16.94
Satellite	9.22	8.78	-0.017	0.93	1.6	29°*	14.97	16.85

*Removed repetitions of 261° in *in situ* data.

Table 7: Data statistics for QuikScat and observations from Bjørnøya.

Data	Mean	Median	Bias	Corr.	<i>Rmsd</i>		P90	P95
	[m/s]	[m/s]	[m/s]		Speed	Direction	[m/s]	[m/s]
<i>In situ</i>	6.79	6.21	-	-	-	-	12.03	13.99
Satellite	7.59	6.79	0.73	0.79	2.81 m/s	44°	13.69	15.44

Table 8: Data statistics for QuikScat and observations from Hopen.

Data	Mean	Median	Bias	Corr.	<i>Rmsd</i>		P90	P95
	[m/s]	[m/s]	[m/s]		Speed	Direction	[m/s]	[m/s]
<i>In situ</i>	5.80	5.60	-	-	-	-	9.76	10.99
Satellite	7.52	6.63	1.72	0.61	4.07 m/s	56°	13.40	16.32

5 Discussion and Conclusions

QuikScat wind data have been validated against *in situ* observations in seven locations on the Norwegian shelf. We obtain a very good correlation for the offshore locations where there is no influence of land on either of the two data types. The lowest correlations are found for the land based stations.

The best statistics is obtained for the comparison at Weather Station M with a correlation of 0.93, an *rms* deviation of 1.6, no mean bias and small differences in the mean and percentile values. For winds above 20m/s there is an overestimation of 1-2m/s from QuikScat, which may be somewhat higher since the wind sensor on Station M is located 16m above sea level.

The comparison against the platform measurements shows similar correlations but here QuikScat is overestimating with a mean bias of 1.1 (Ekofisk) and 1.76 (Gullfaks-C). The original data from sensor level and the reduced 10m data at Gullfaks-C are compared with QuikScat winds in Figure 10.

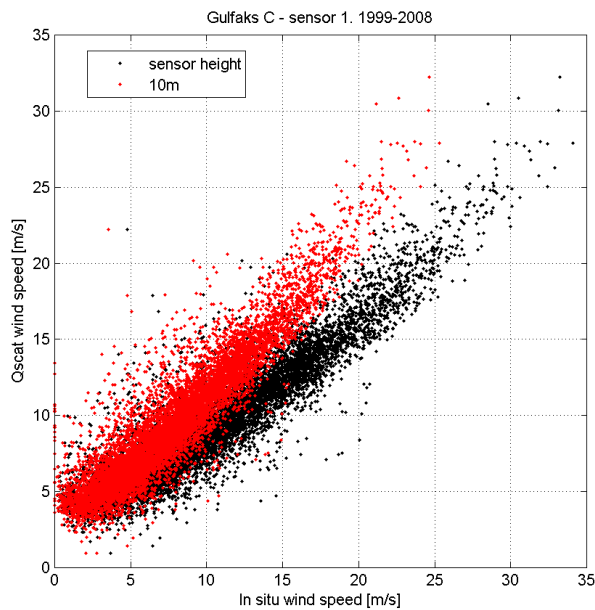


Figure 10: Scatter plot of wind speed from Gullfaks-C at sensor level of 143m (black) and reduced to the 10m level (red), compared to QuikScat, representative of 10m. The red points are thus the same as presented in Figure 2 a).

Wind speed at sensor height is operationally reduced to 10m above sea level by means of a formula based on the logarithmic wind profile

$$U_{10} = U \left(\frac{10}{z} \right)^{0.13}$$

where z is the sensor level measured in meters above sea level and U [m/s] is the 10-minute average of the wind speed as measured at sensor level. This relation is known to be inaccurate and work is needed to improve it. The data analysed here indicates that the Ekofisk and Gullfaks-C winds are reduced too much since we here get a positive bias of 1.1m/s and 1.7m/s which is not observed at Station M.

Compared to buoy measurements QuikScat has a large positive bias at high wind speeds. The buoys used for validation in this study have been in operation during 9 month. The maximum wind speed measured on any of the two buoys during this time is only 15.4m/s. It may suggest that the wind measurements on the buoys have problems in bad weather, for instance due to high waves and sea

spray. The measurements are furthermore obtained at 3.5m a.s.l. and therefore should be generally lower than QuikScat measurements representative of 10m height.

The poorest results are found when validating against the land based stations. When comparing satellite wind with a land station we need to select an offshore reference point. This introduces a significant source of error for to two main reasons. One is the distance between the *in situ* location and the QuikScat point of 48km and 30km for Bjørnøya and Hopen, respectively. The other being that the *in situ* data typically are affected by the topography while QuikScat measures oceanic wind conditions.

The *in situ* data from Weather Station M are most useful for validation of satellite data of those analysed here. At Station M the wind sensor is placed on a relatively small construction (the weather ship *Polarfront*) at comparable height to the QuikScat 10m level and it provides a long time series covering the whole QuikScat period. For this site the rms deviation is comparable to those reported by others validating against buoys and ships (Bourassa et al., 2003; Chelton and Freilich, 2005). The rms deviation for the wind direction is somewhat higher at Station M, which may be caused by the high low pressure activity in the Norwegian Sea (Draper and Long, 2002).

In summary, scatterometer data surely gives high quality wind observations, superb to e.g. buoy in terms of coverage. For the data sets analysed here QuikScat winds are generally higher than *in situ* data for high wind speeds. Some of this difference we assign to underestimation in the *in situ* observations (in the case of buoys) and possibly too strong reduction of the platform winds (Ekofisk and Gullfaks-C). At the islands, high wind values from QuikScat may be due to ice contaminated grid cells. Apart from this, we estimate that we are left with an overestimation of QuikScat winds of 1-2m/s for wind speeds above ~20m/s, but this has not been investigated in detail.

Scatterometer data are available back to 1991 (ERS-1) and are suitable for regional wind climate studies. Efficient ways to utilize scatterometer data for investigations of regional wind climate will be:

- 1) Use the data to validate numerical weather prediction (NWP) reanalysis (rerun of NWP models) as e.g. HIRLAM atmosphere model in the met.no wind and wave hindcast archive.
- 2) Assimilate the scatterometer data in the NWP reanalysis.

A correction of atmospheric stability may be carried out using sea surface temperature from satellite and air temperature from the observation sites. In areas where ice may be present, careful filtering of ice contaminated data is needed.

Acknowledgements

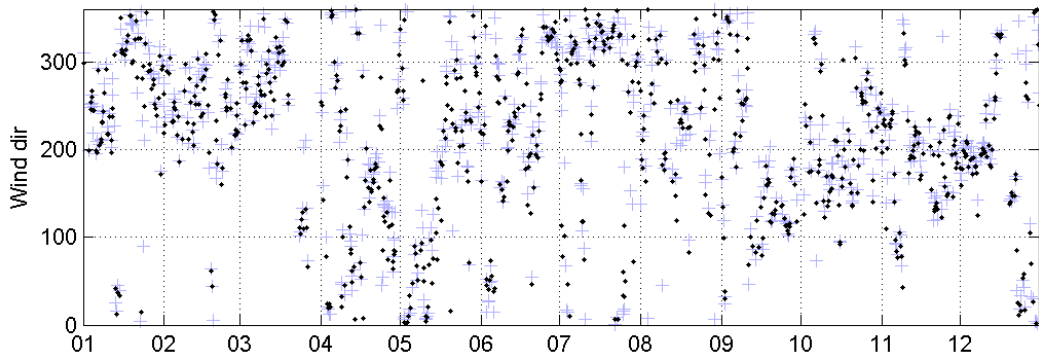
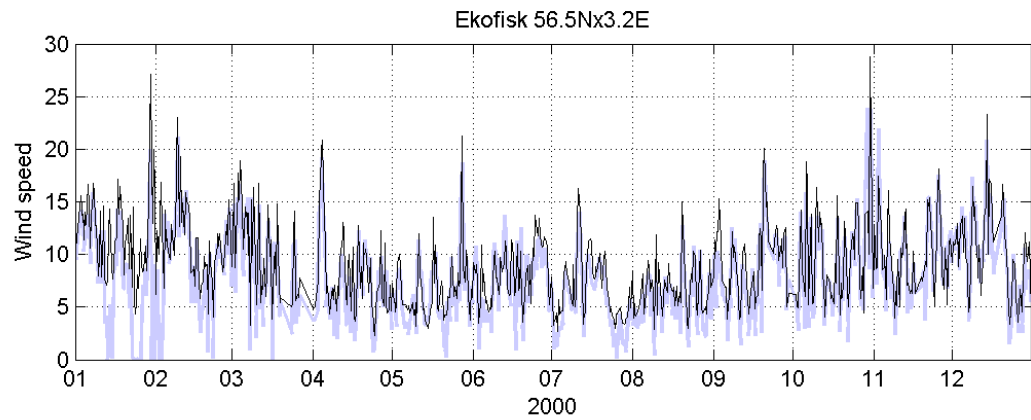
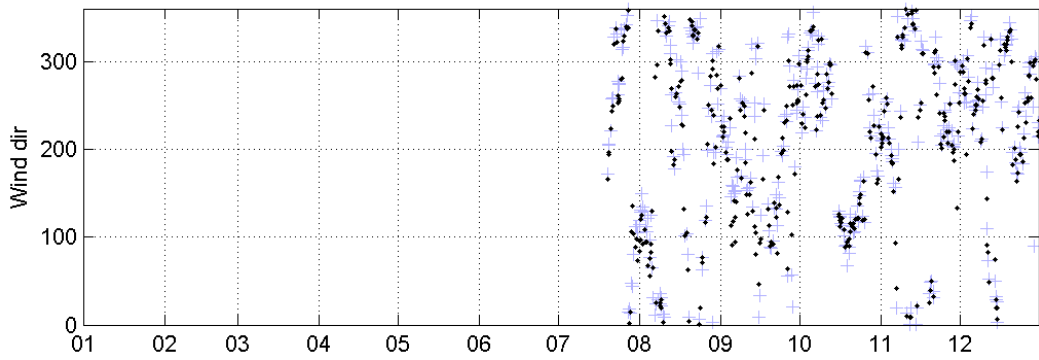
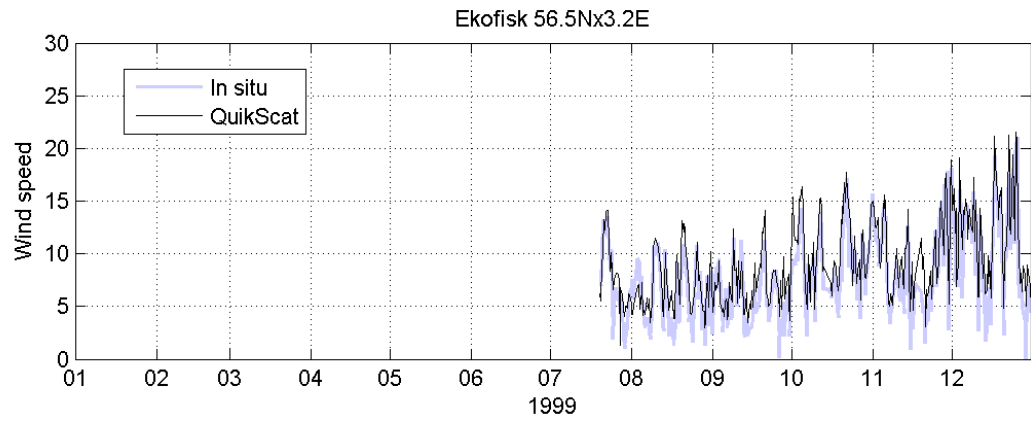
The SeaWinds on QuikSCAT Level 2B Ocean Wind Vectors 25 Km Swath data were obtained from the Physical Oceanography Distributed Active Archive Center (PO.DAAC) at the NASA Jet Propulsion Laboratory, Pasadena, CA. <http://podaac.jpl.nasa.gov>.

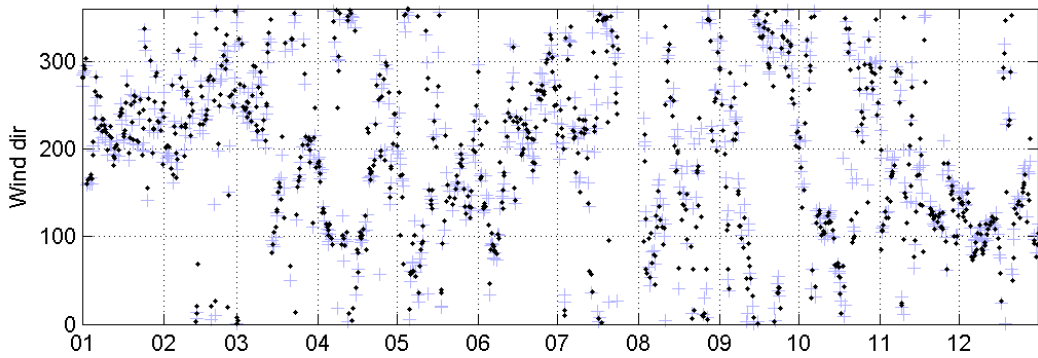
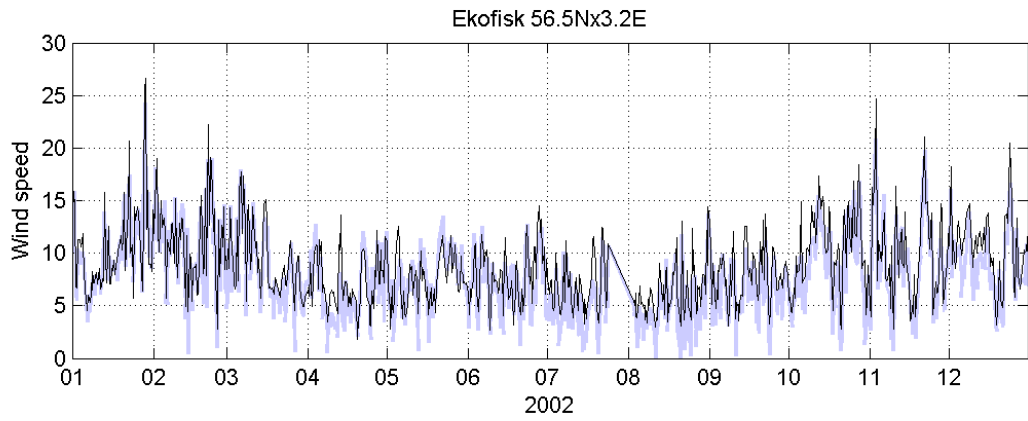
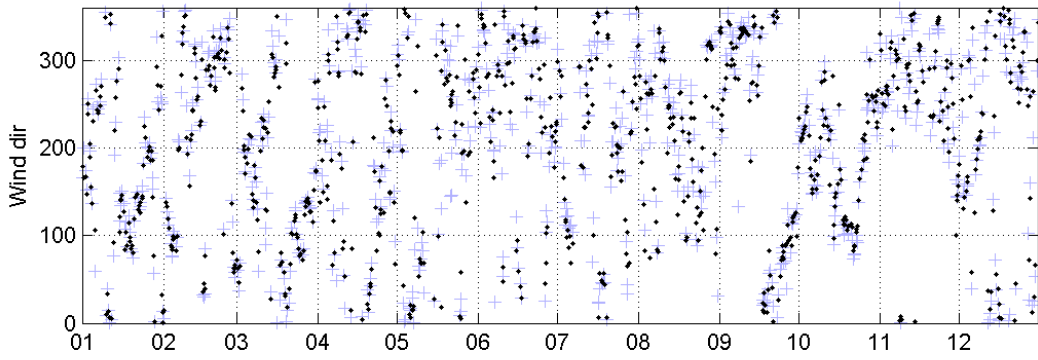
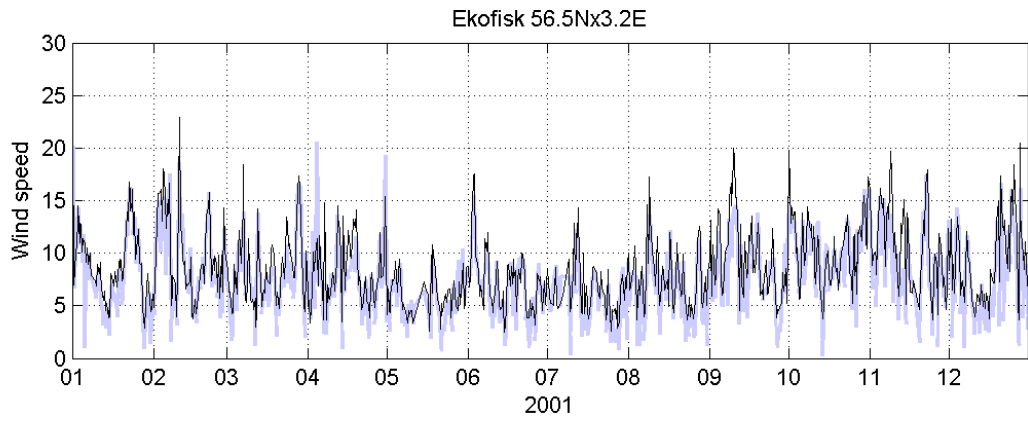
References

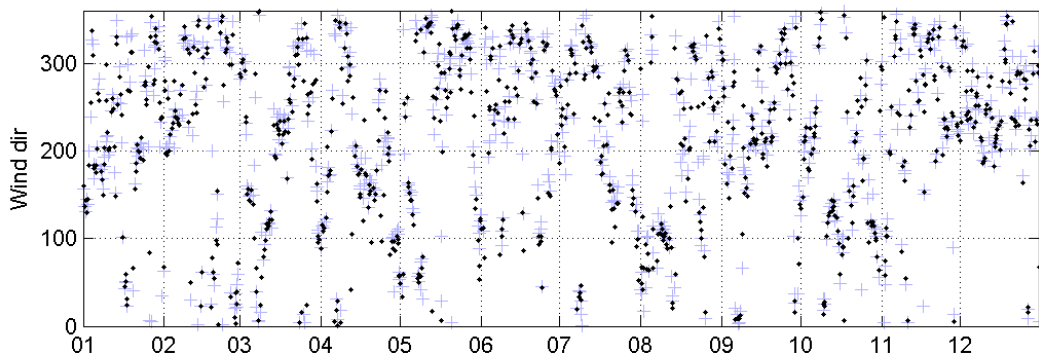
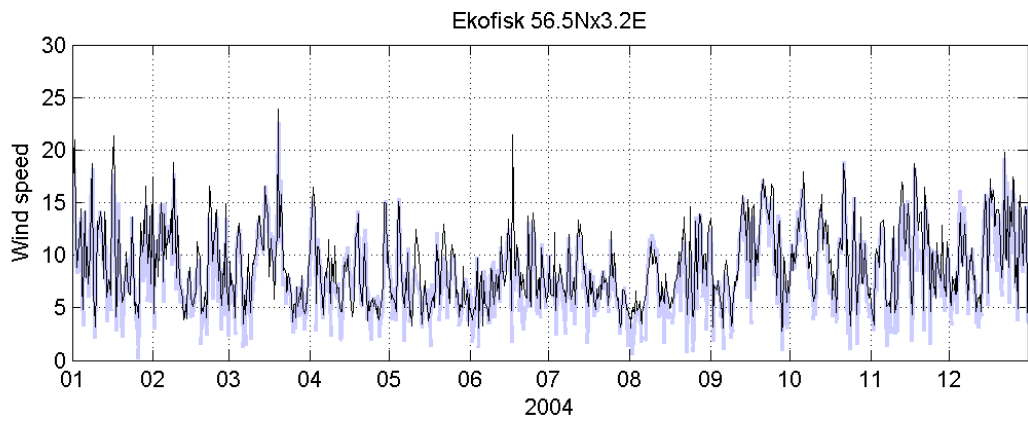
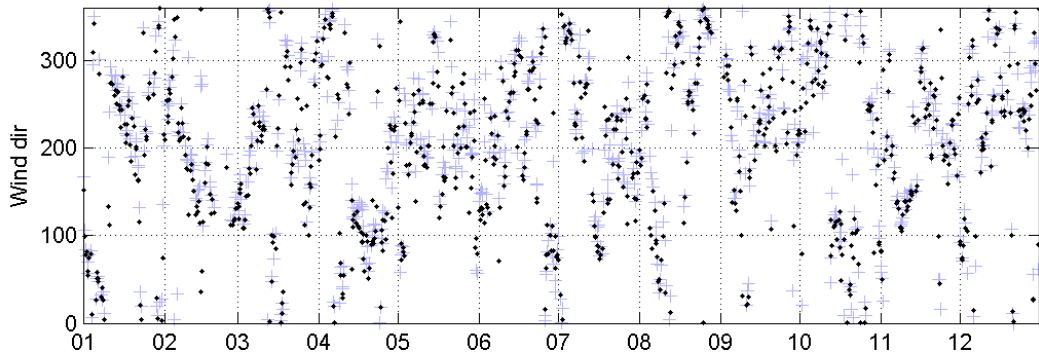
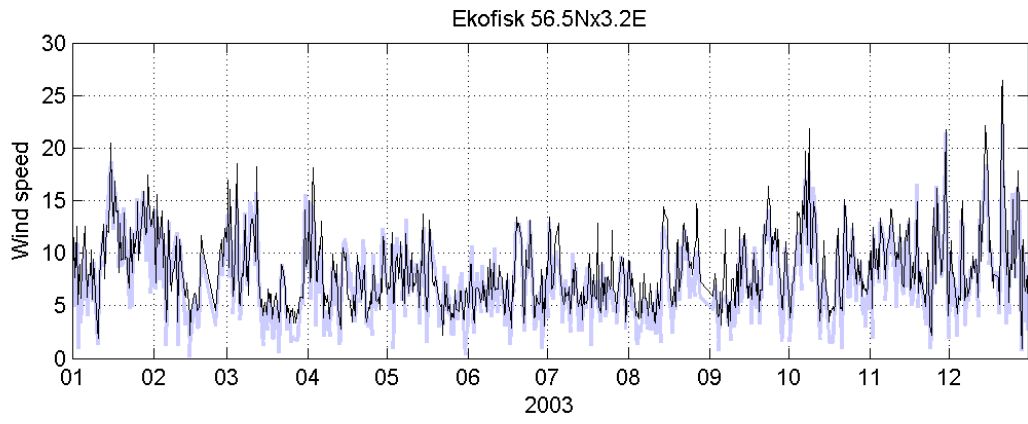
- Bourassa, M. A., D. Legler, J. J. O'Brian and S. R. Smith (2003) SeaWinds validation with research vessels, *Journal of Geophysical Research*, 108, C2, 3019.
- Breivik, L.A. (1993) Assimilation of ERS-1 scatterometer wind information in a limited area model. *DNMI Technical report no. 104*.
- Breivik, L.A. and Baard Haugse (1994) Scatterometer wind retrieval at the Norwegian Meteorological Institute. *DNMI Technical report no. 124*.
- Chelton, D. B., and M. H. Freilich (2005) Scatterometer-based assessment of 10m wind analysis from the operational ECMWF and NCEP numerical weather prediction models, *Monthly Weather Review*, 133, 409-429.
- Draper, D., and D. Long (2002) An assessment of SeaWinds on QuikScat wind retrieval, *Journal of Geophysical Research*, 107, C12, 3212.
- Furevik, B. R., R. Barthelmie, A. M. Sempreviva, B. Jimenez (2006) Offshore wind energy potential in the Mediterranean using satellite scatterometer data, *Presented at OWEMES 2006*, Civitavecchia (Rome), Italy, April, 20-22.
- Liu, W. T., and W. Tang (1996) Equivalent neutral wind, *JPL Publication 96-17*, Jet Propulsion Laboratory, California Institute of Technology.
- Schyberg and Breivik (2002) Objective analysis combining observation errors in physical space and observation space, *Q.J.R.Meteorol.Soc.*, Vol 128 pp. 695-711.
- Tveter F. (2002) The DNMI QuikScat wind-vector nowcasting product, *DNMI Research Note no. 71*.
- Tveter, F. (2006) Assimilating ambiguous QuikScat scatterometer observations in HIRLAM 3-D-Var at the Norwegian Meteorological Institute, *Tellus*, 58A, 5968.
- QuikScat Science data product, User's Manual, Overview and Geophysical Data Products, Version 3.0, Jet Propulsion Laboratory, California Inst. Of Tech., Edited by T. Lungu, September 2006.

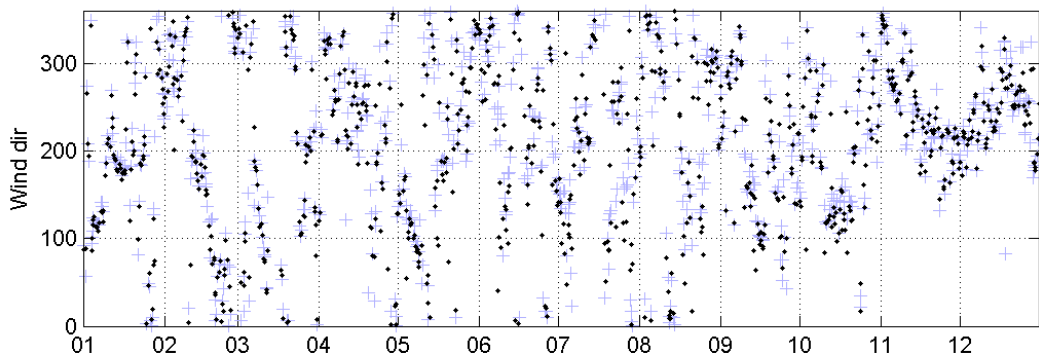
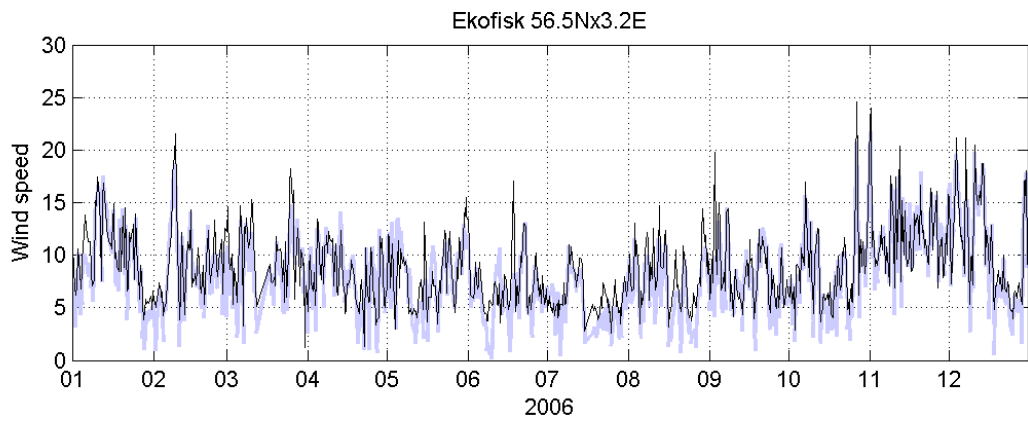
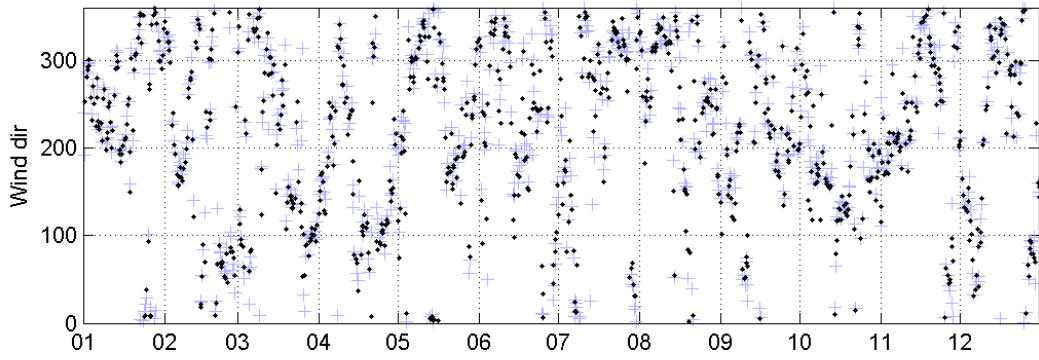
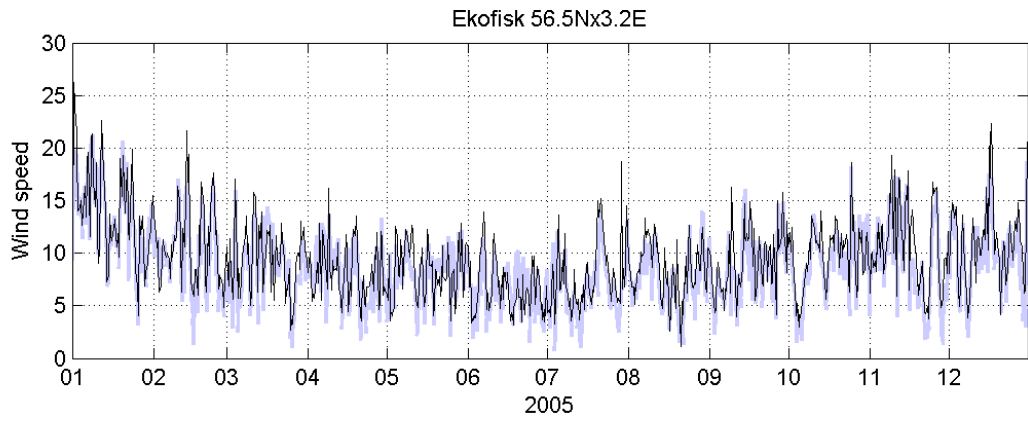
6 Appendix

6.1 Ekofisk – Sensor 1

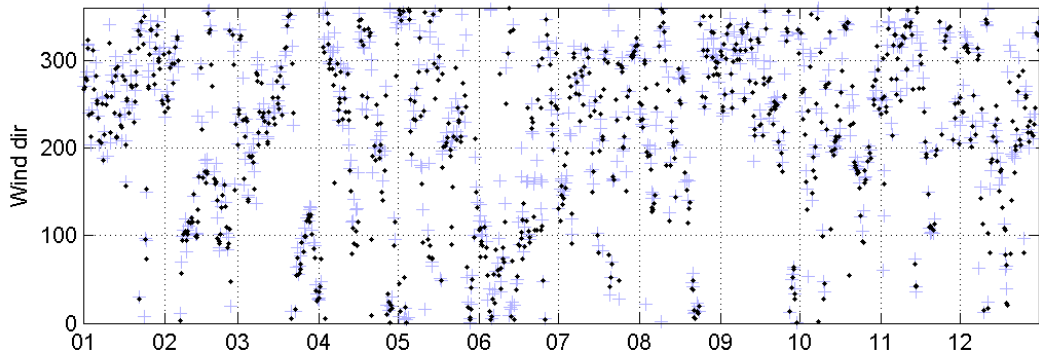
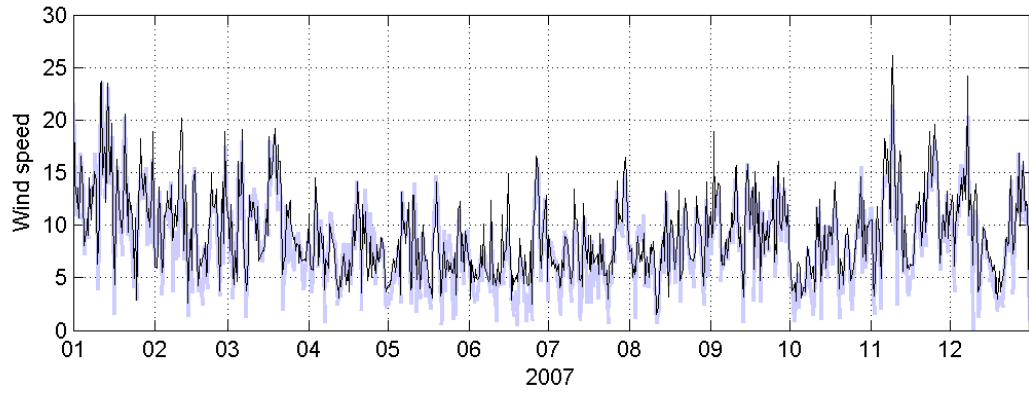




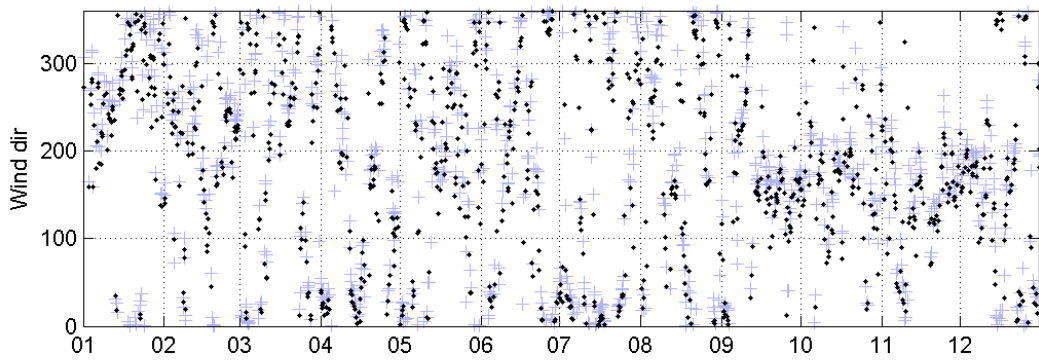
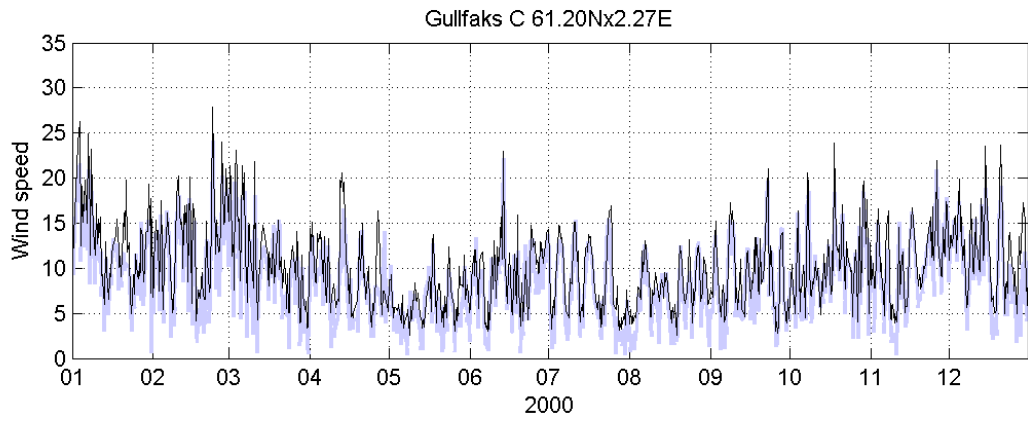
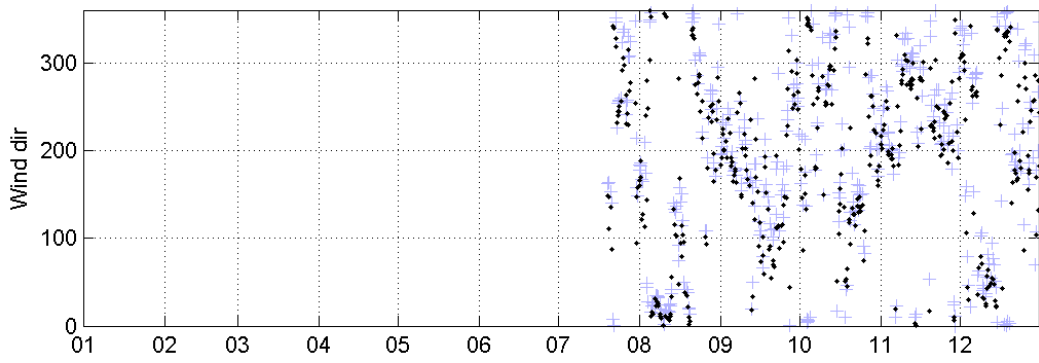
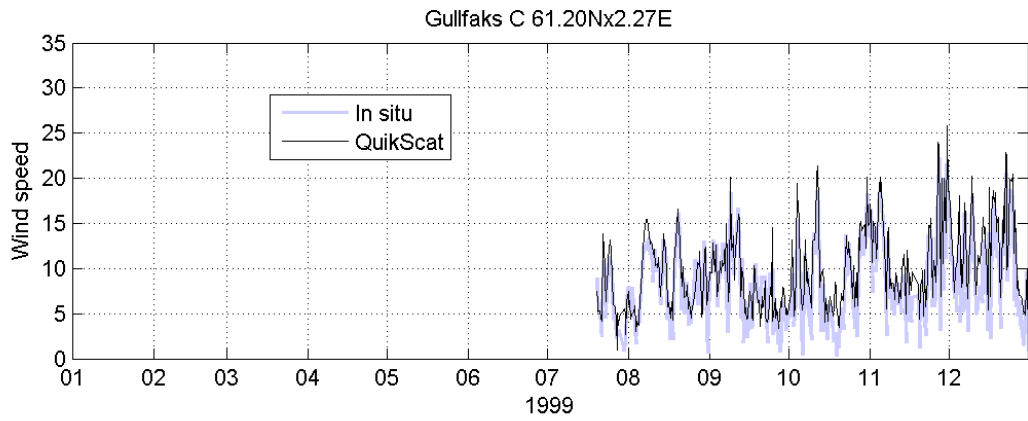


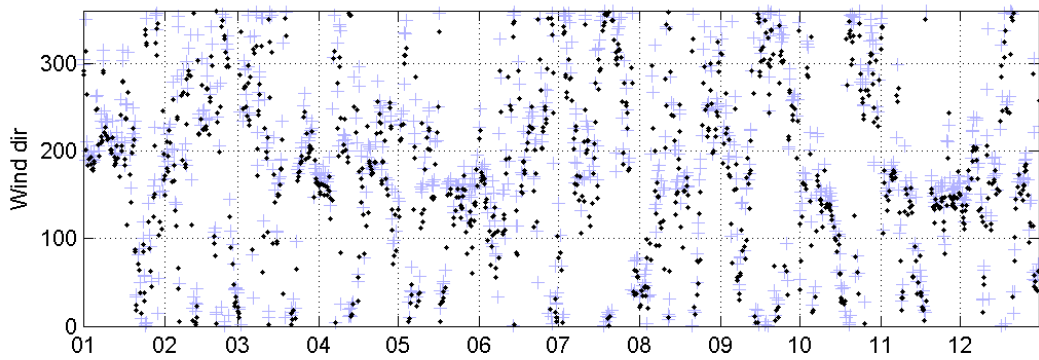
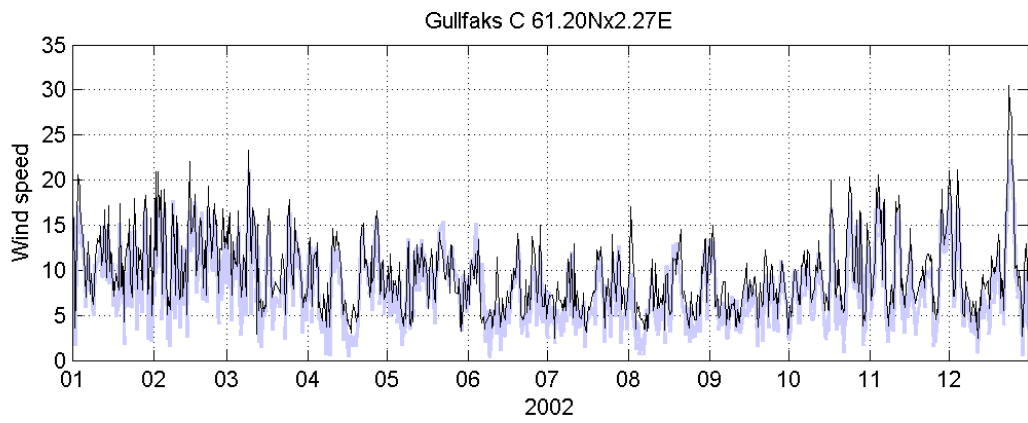
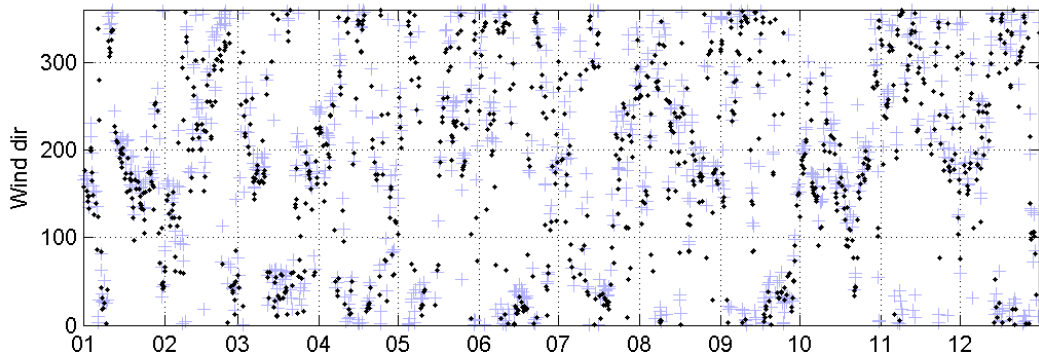
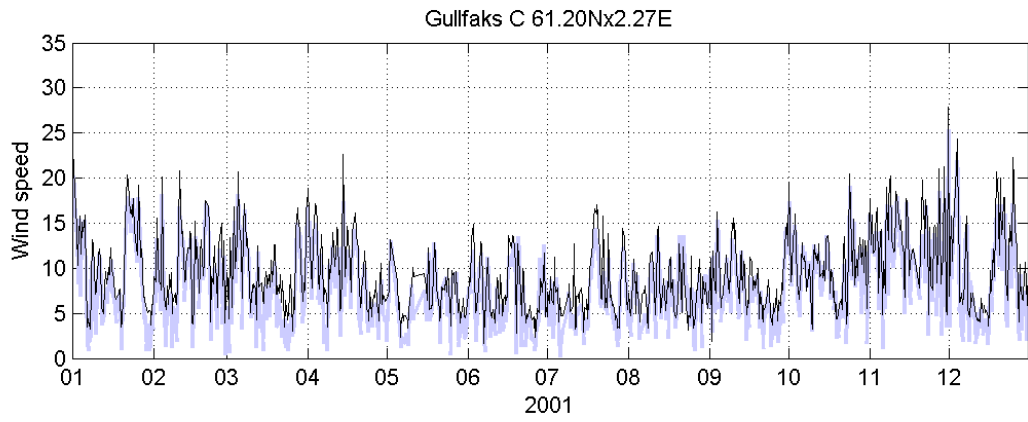


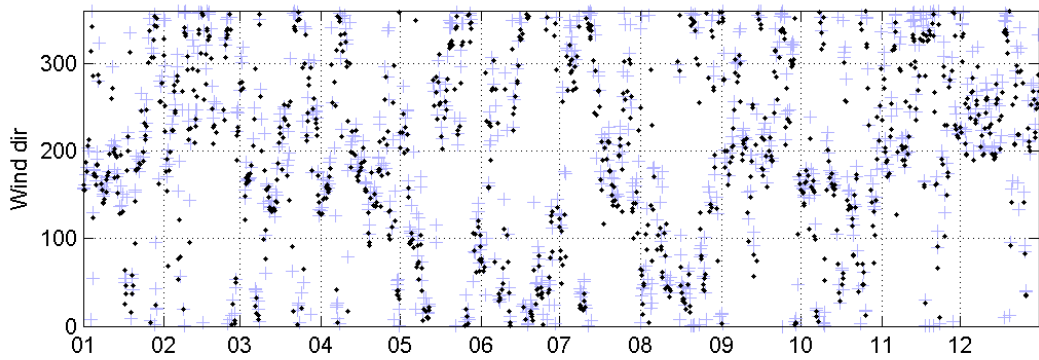
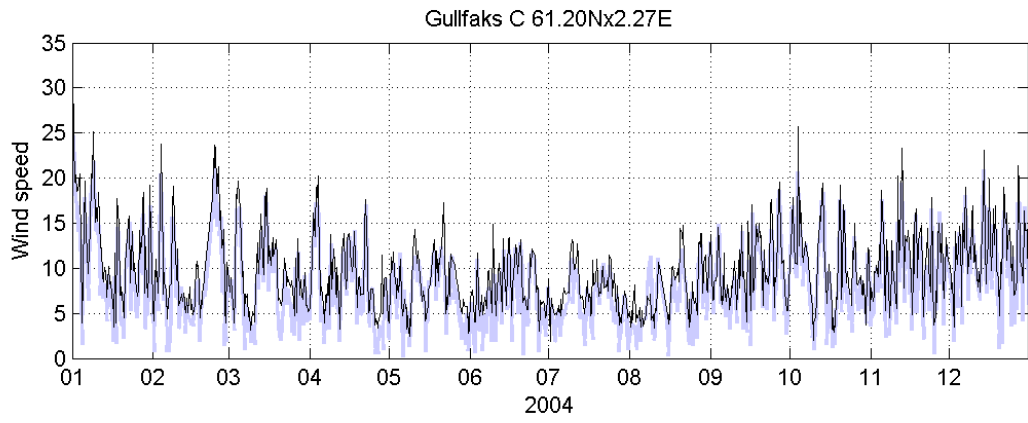
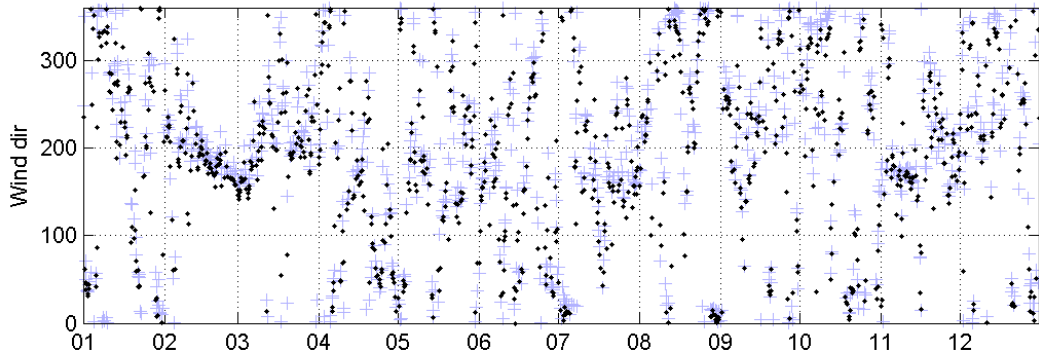
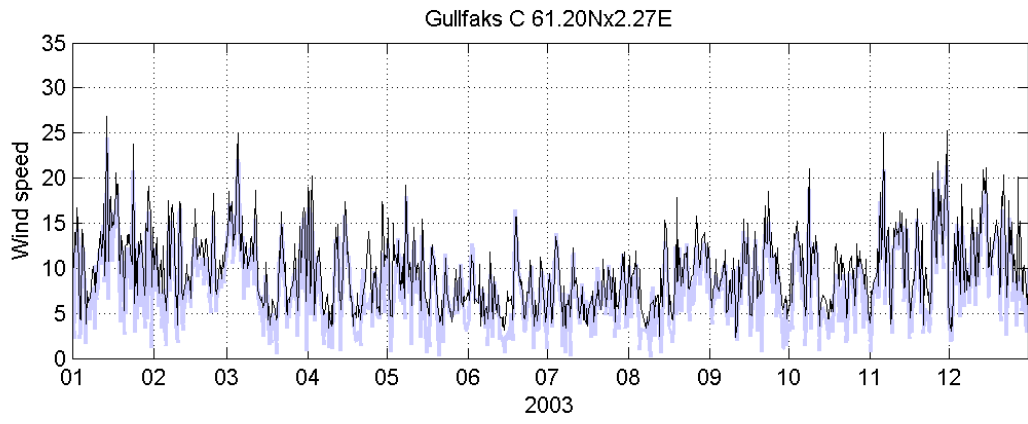
Ekofisk 56.5Nx3.2E

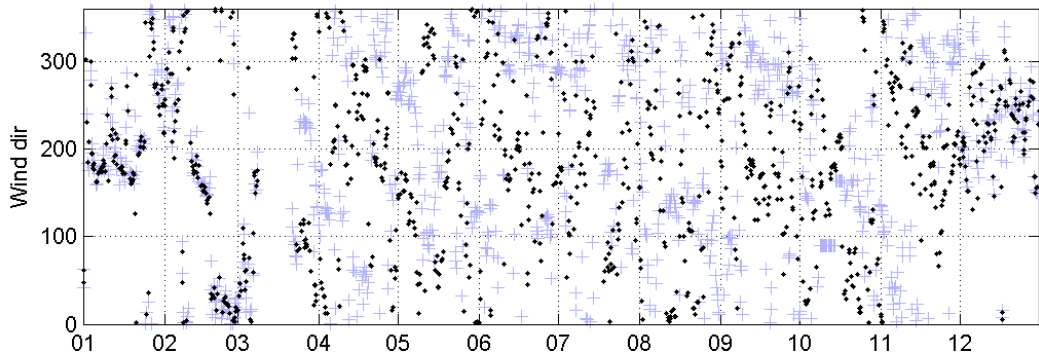
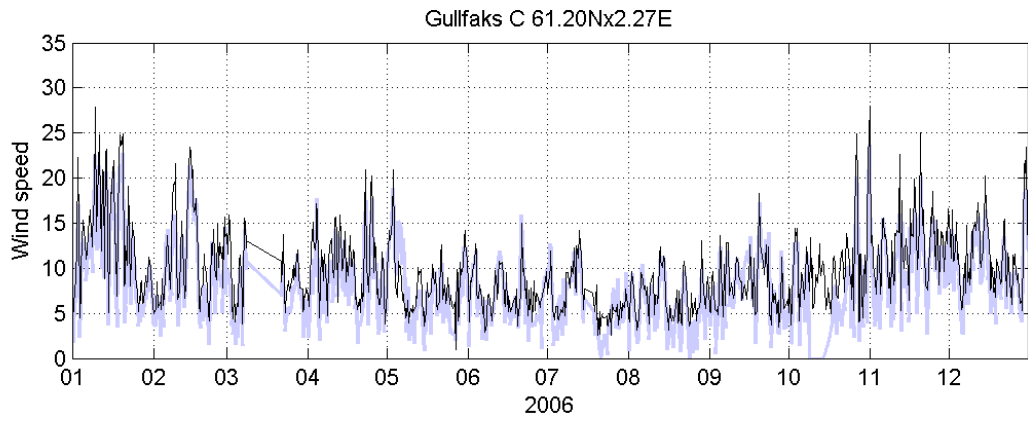
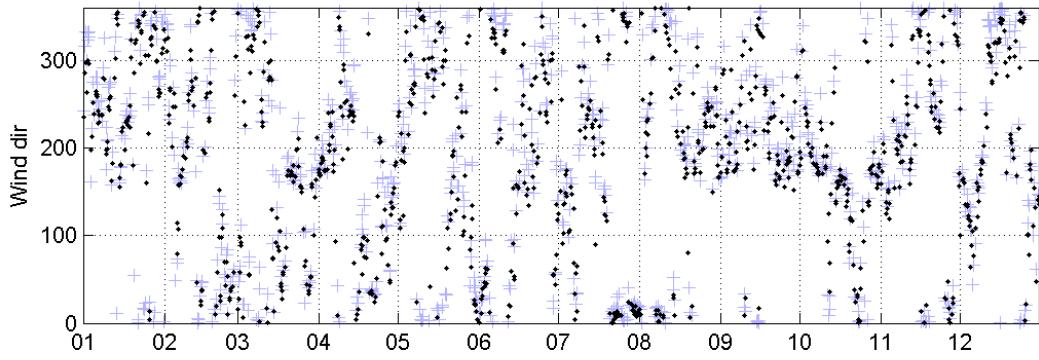
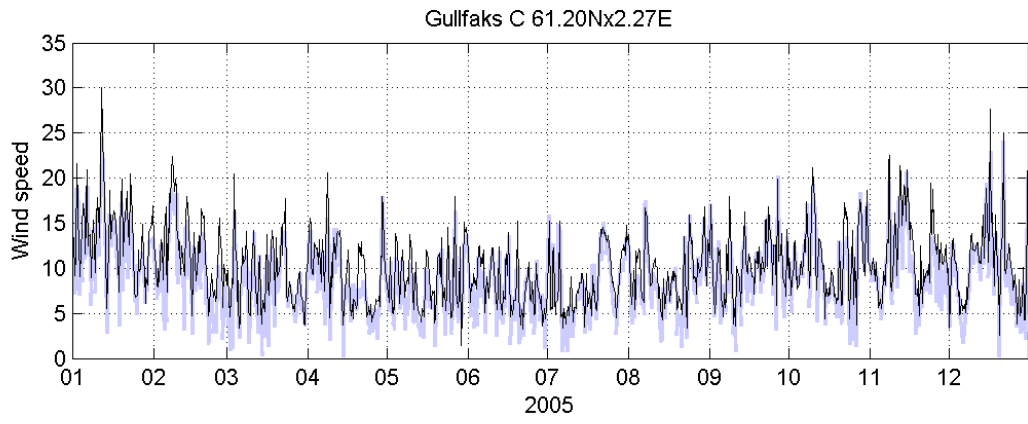


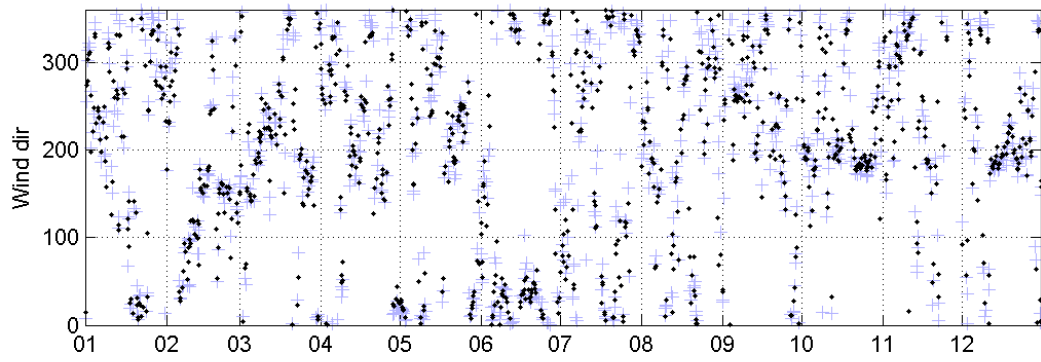
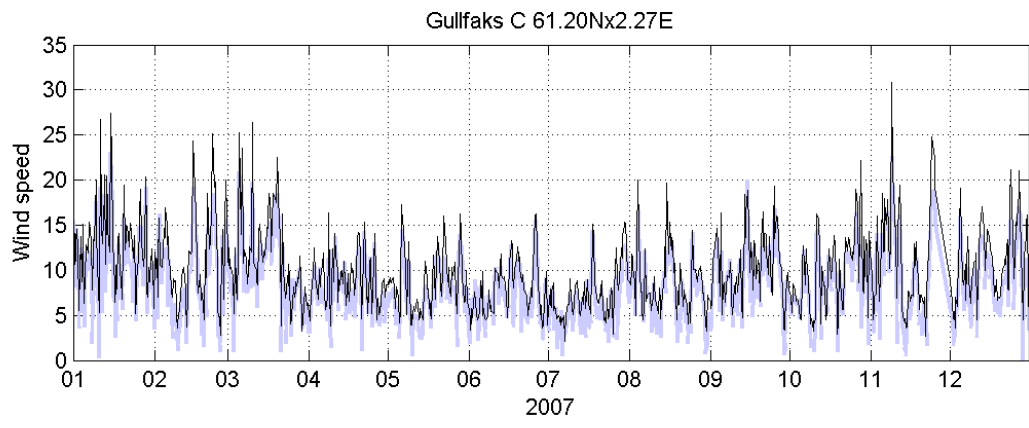
6.2 Gullfaks-C – Sensor 1



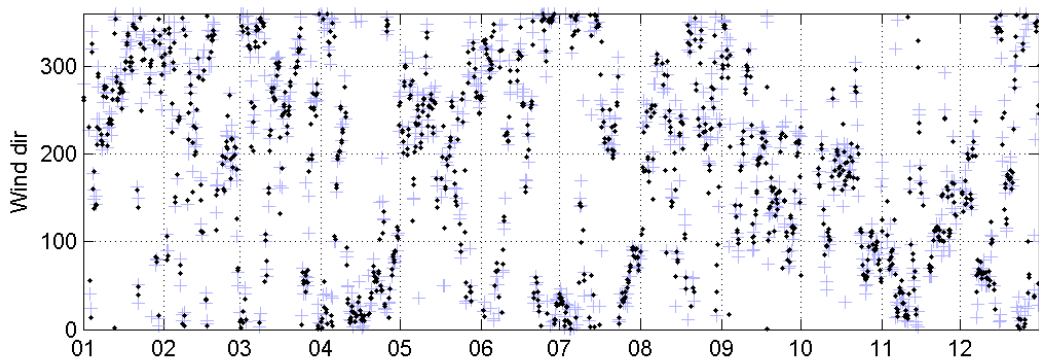
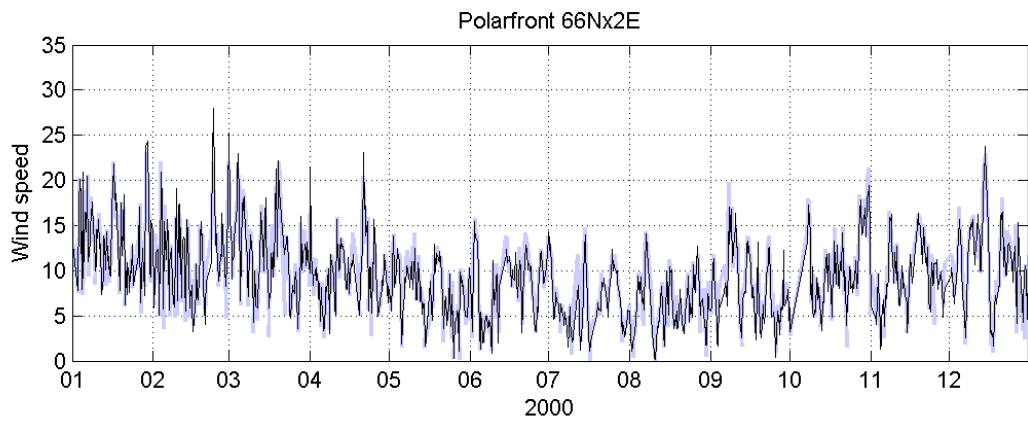
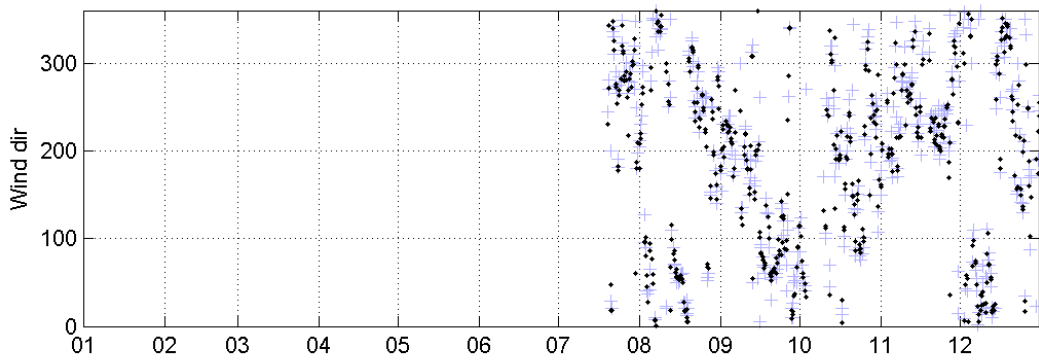
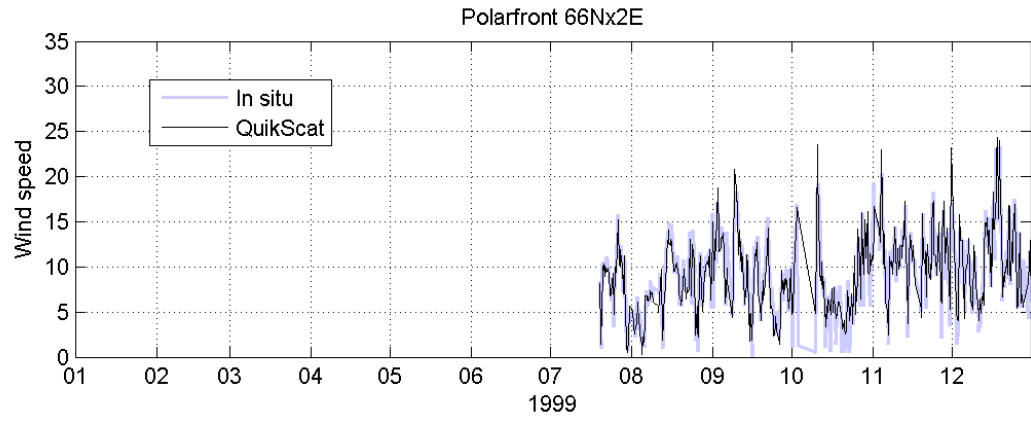


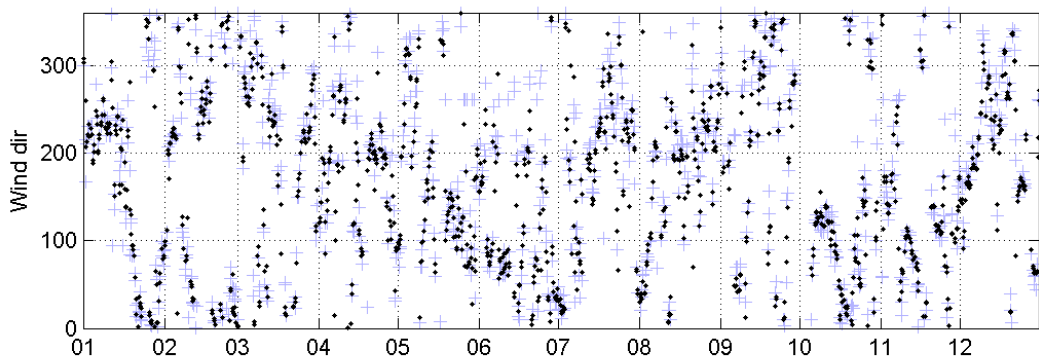
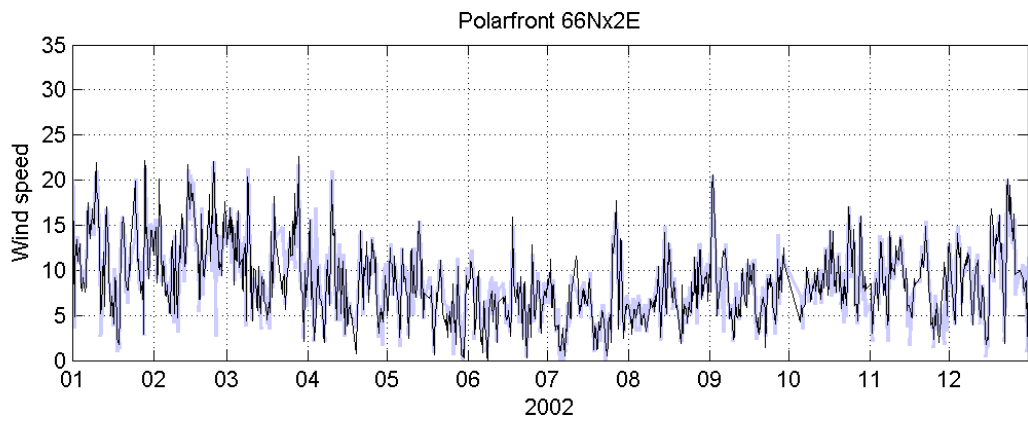
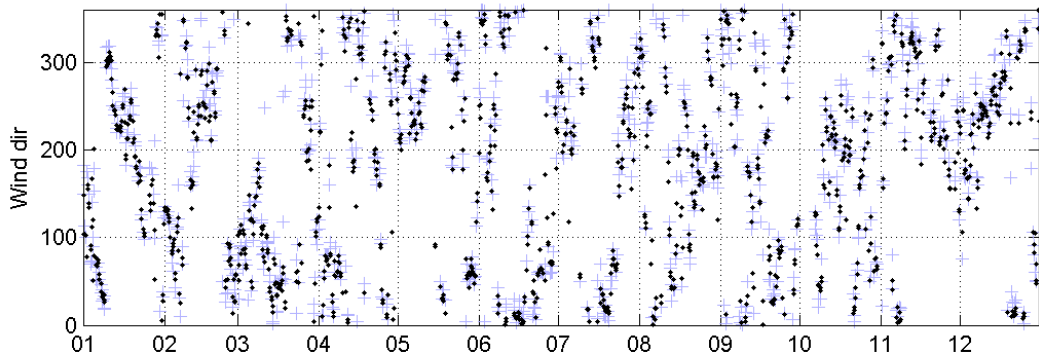
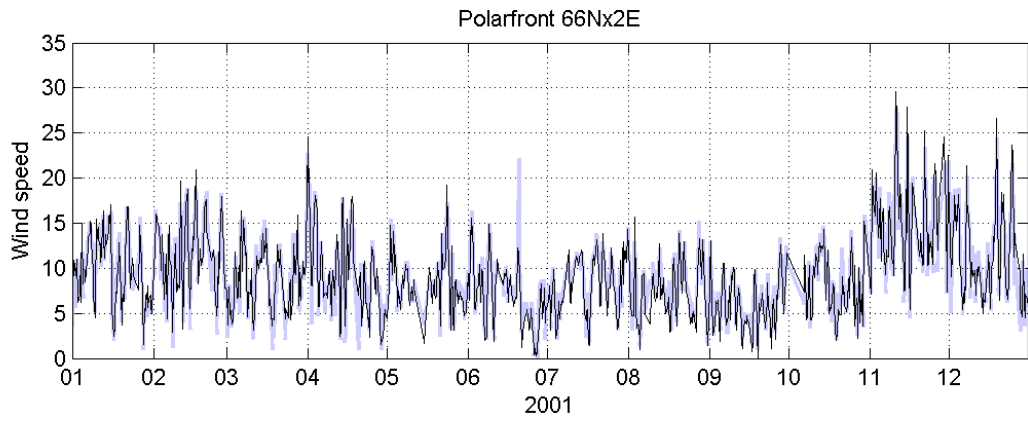


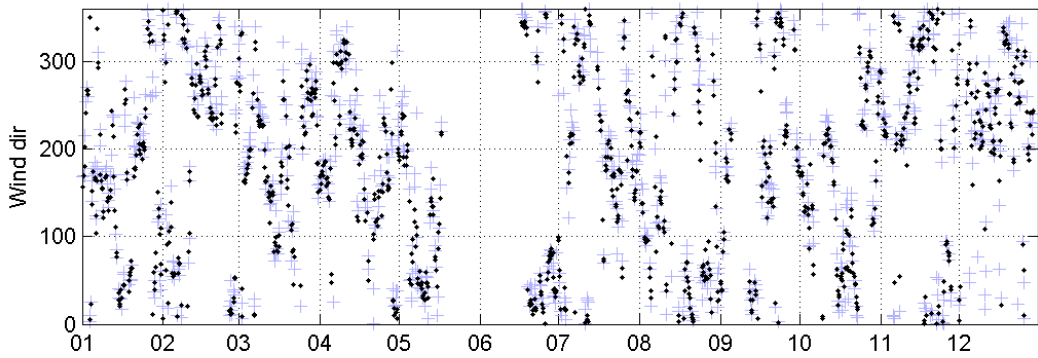
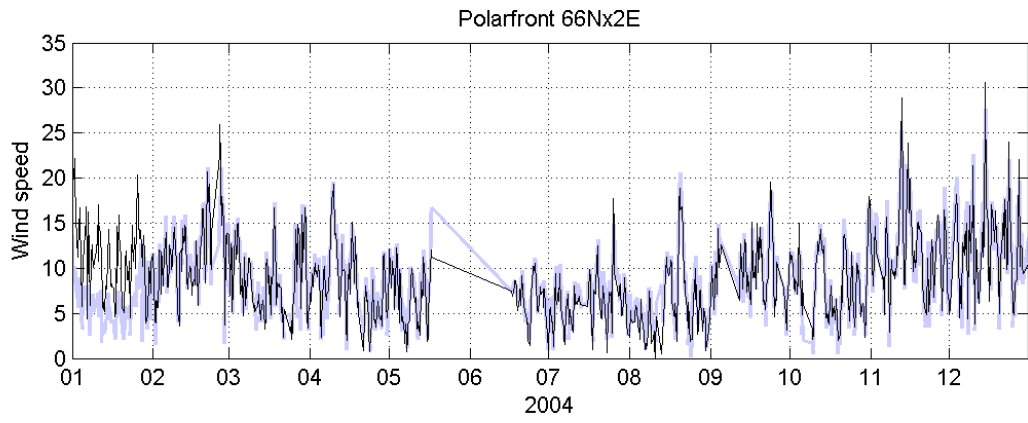
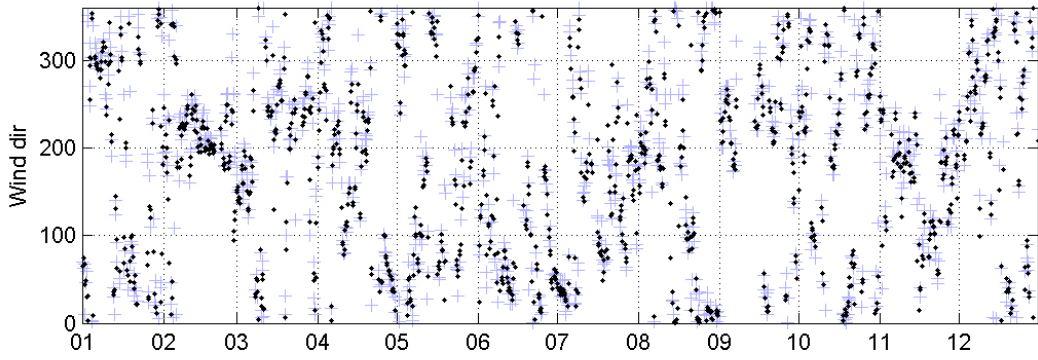
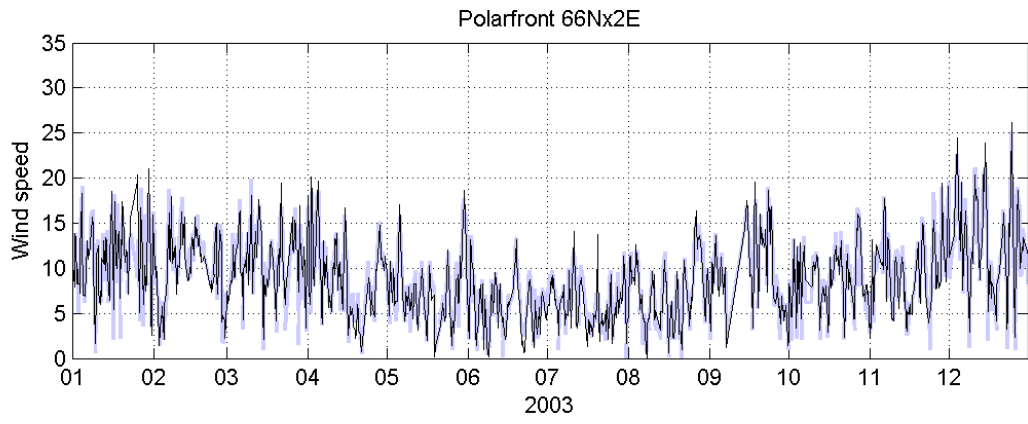


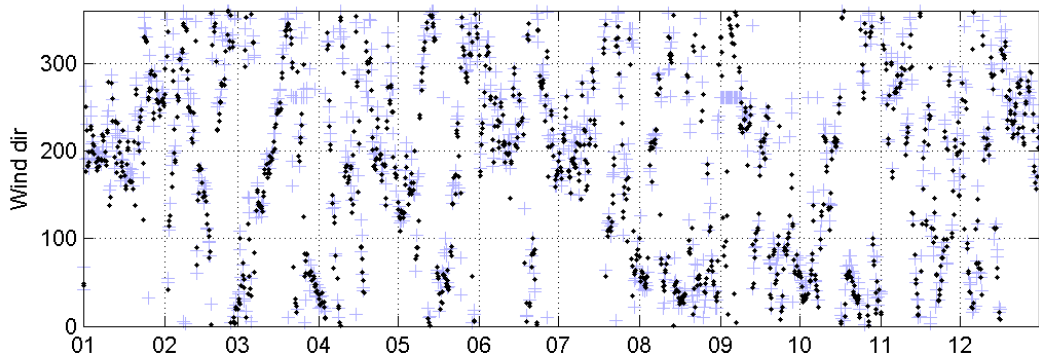
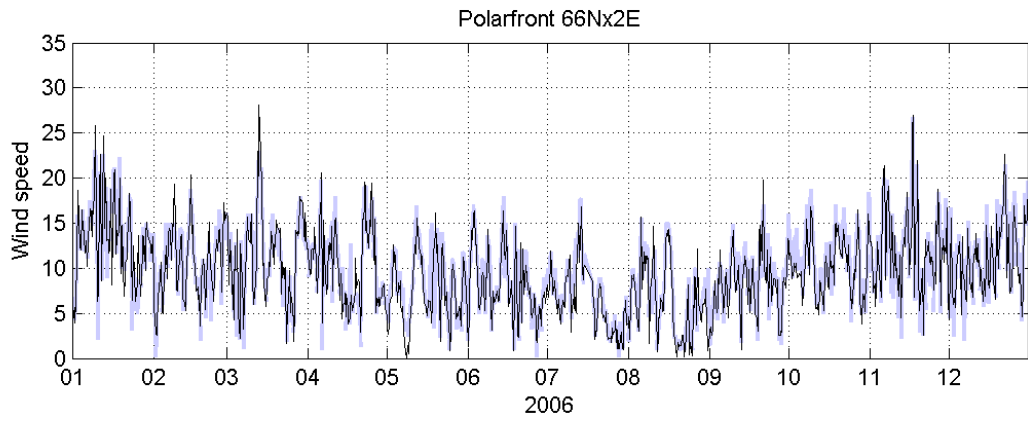
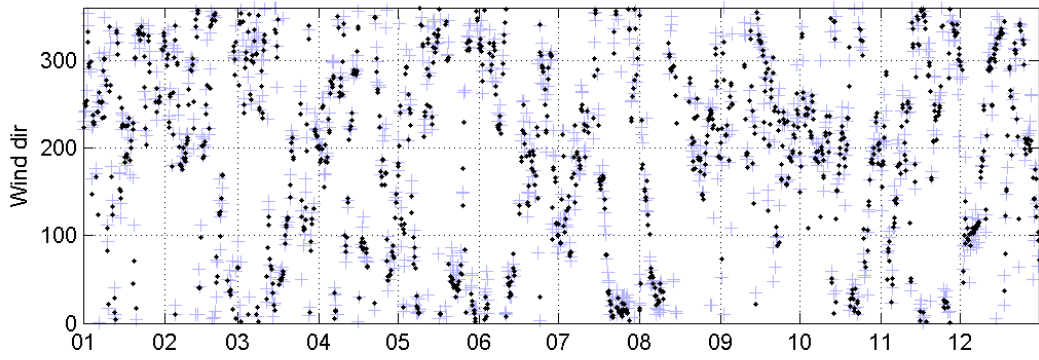
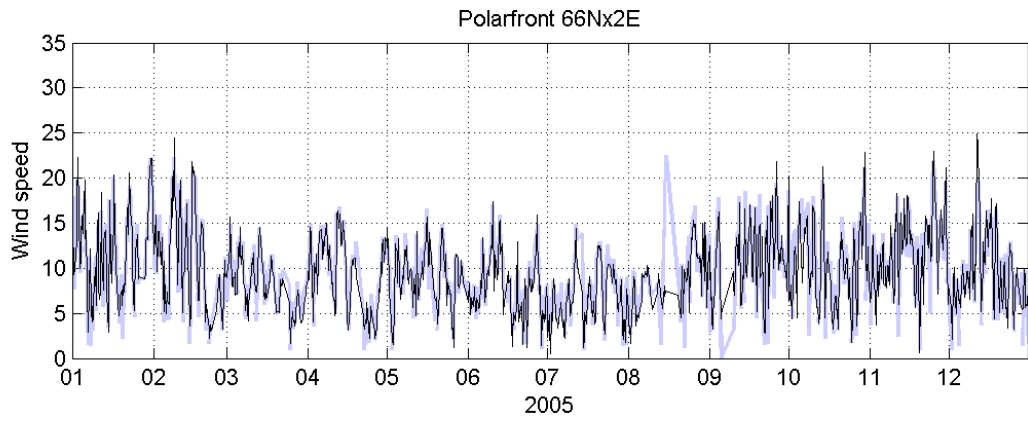


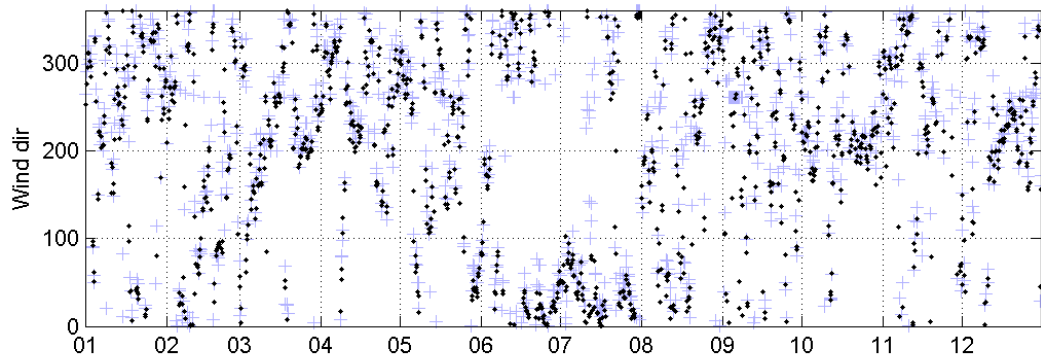
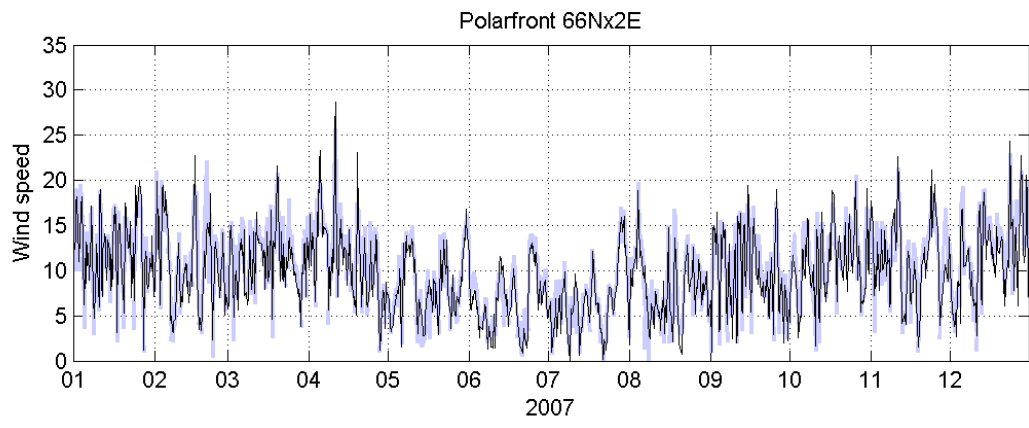
6.3 Weather Station M



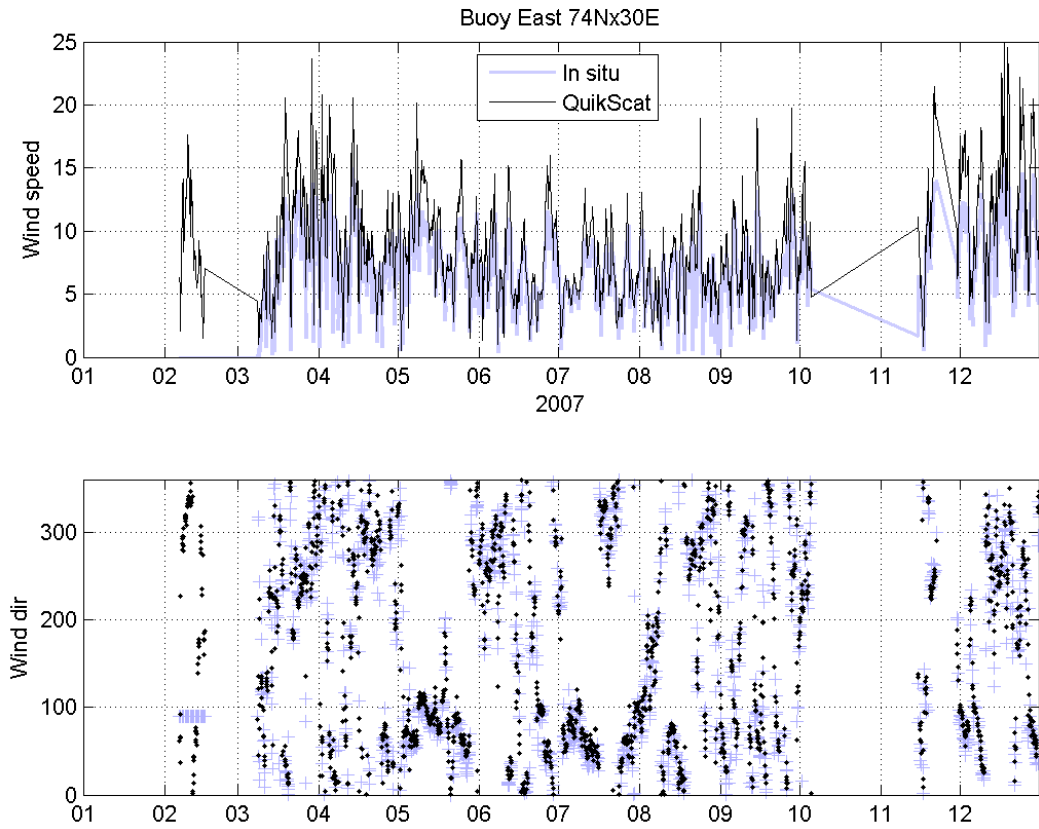




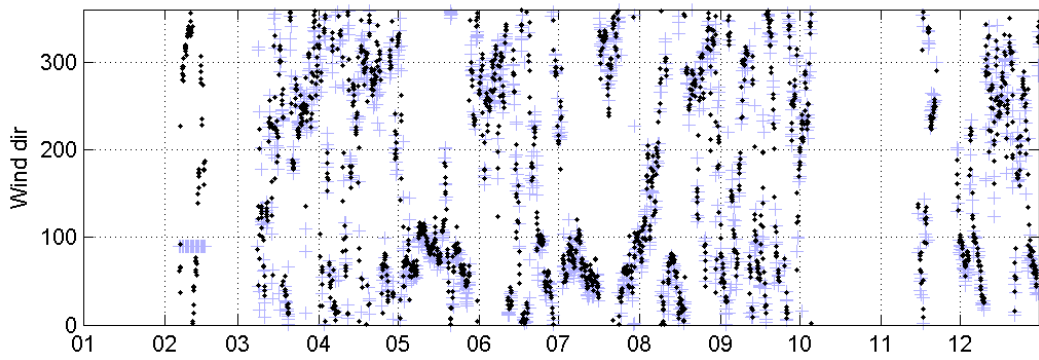
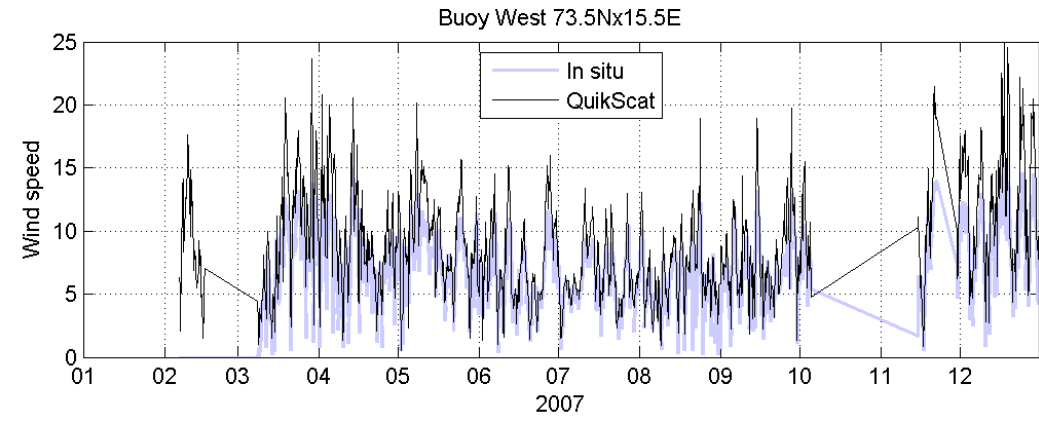




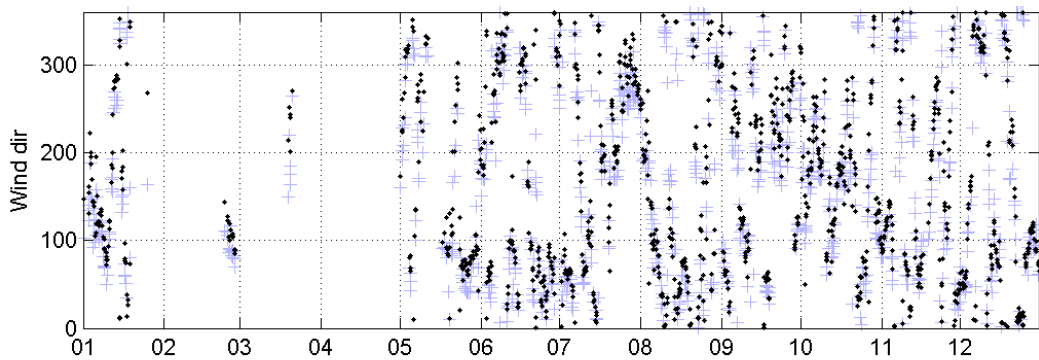
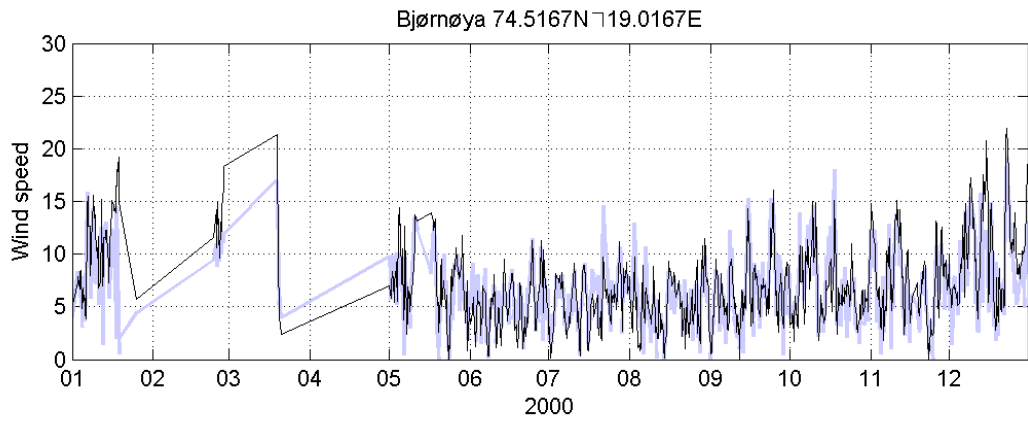
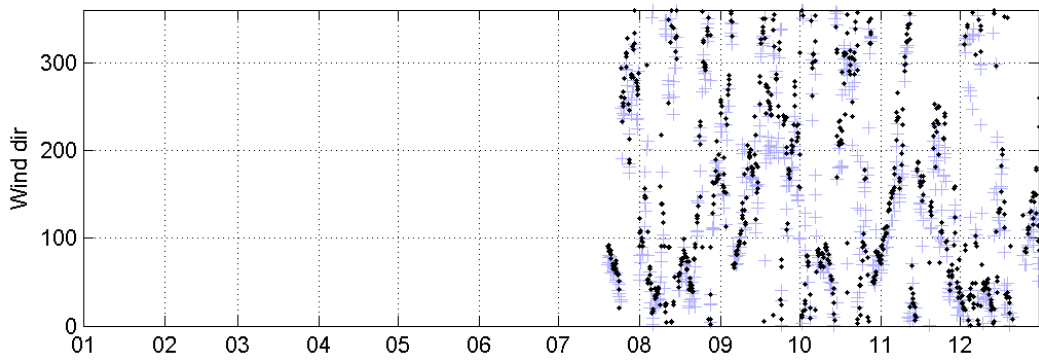
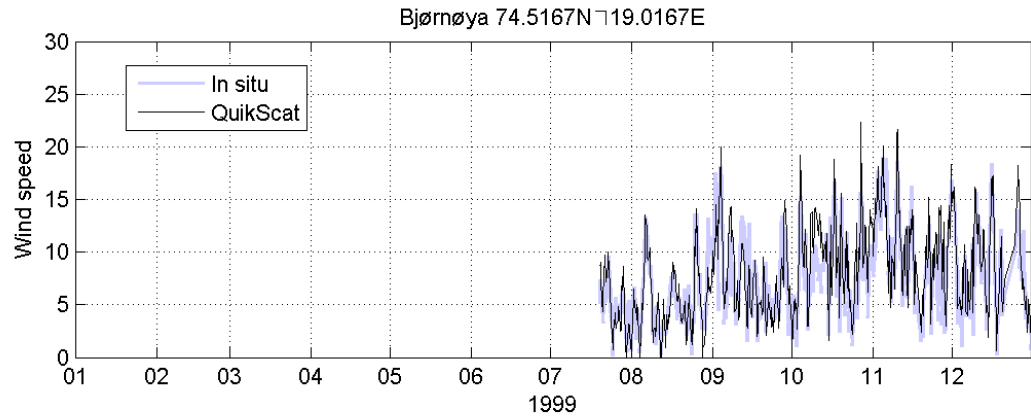
6.4 Barents Sea Buoy East

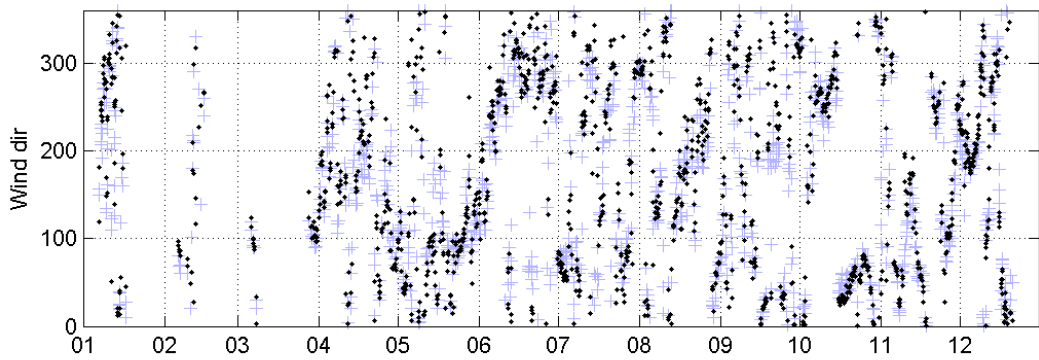
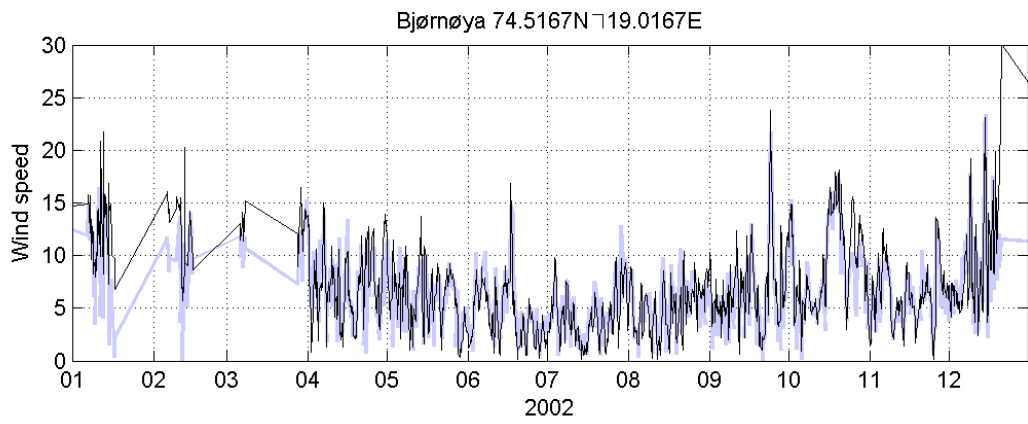
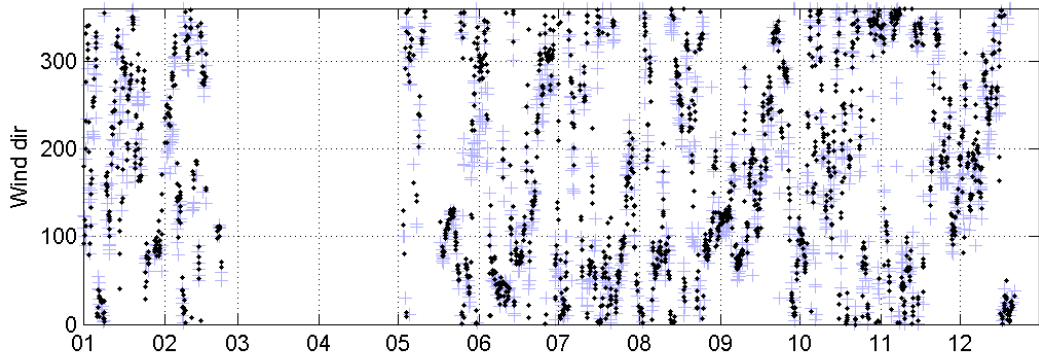
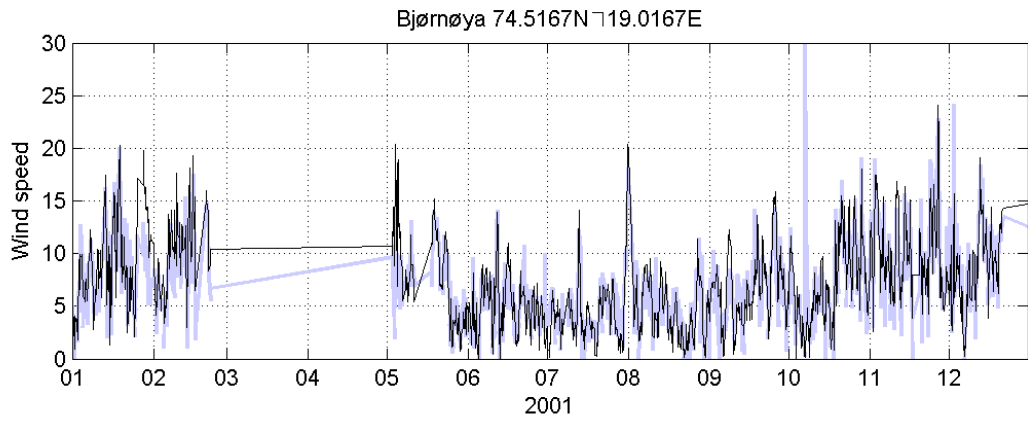


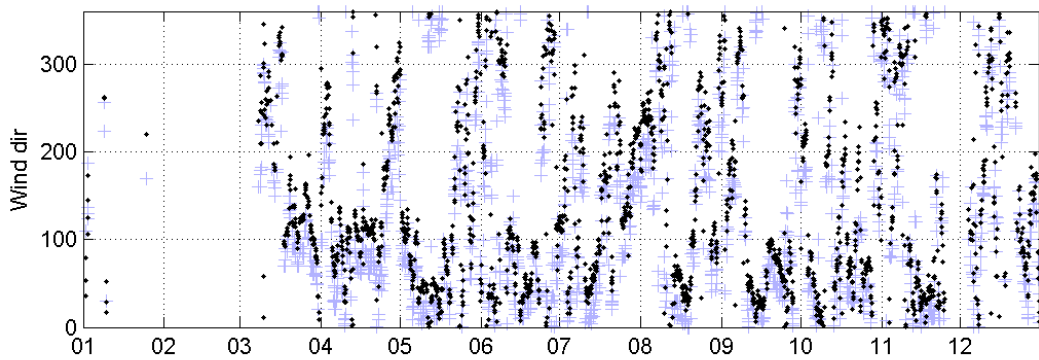
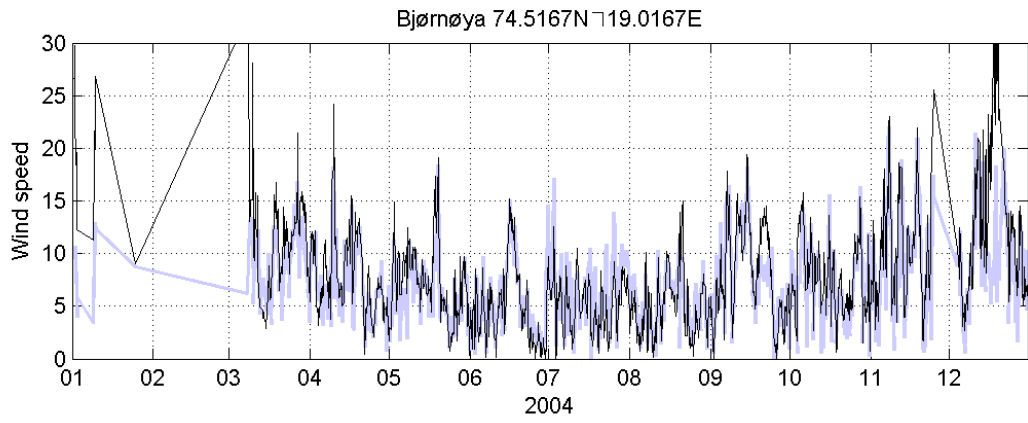
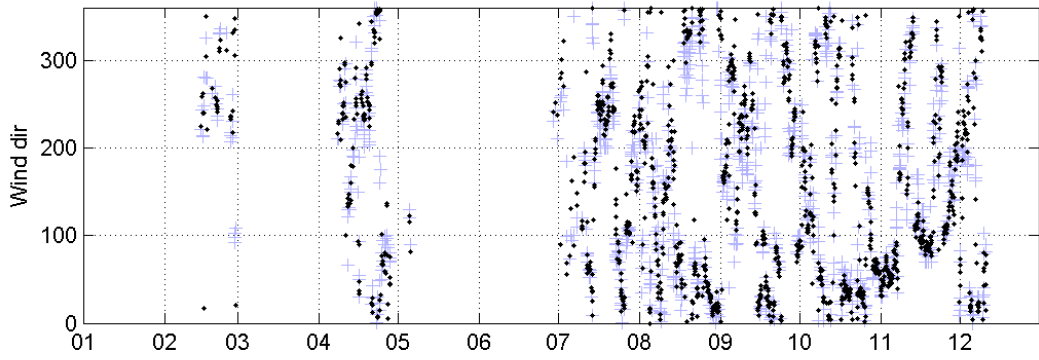
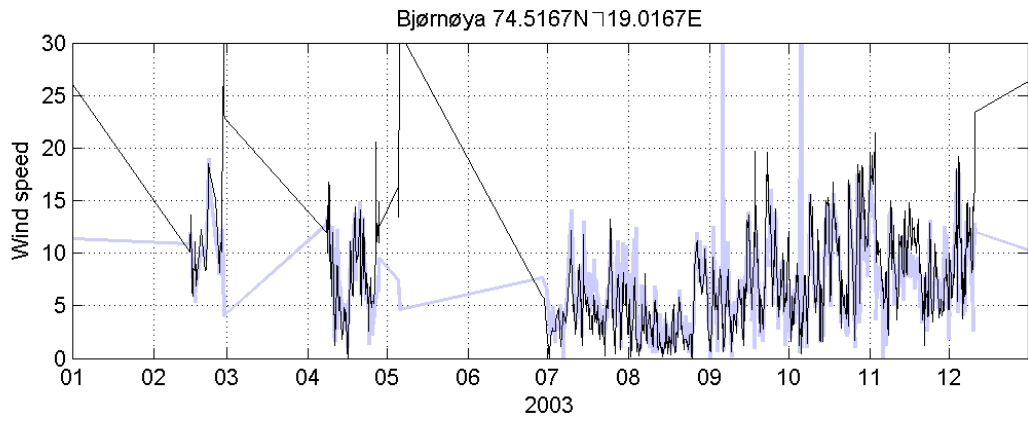
6.5 Barents Sea Buoy West

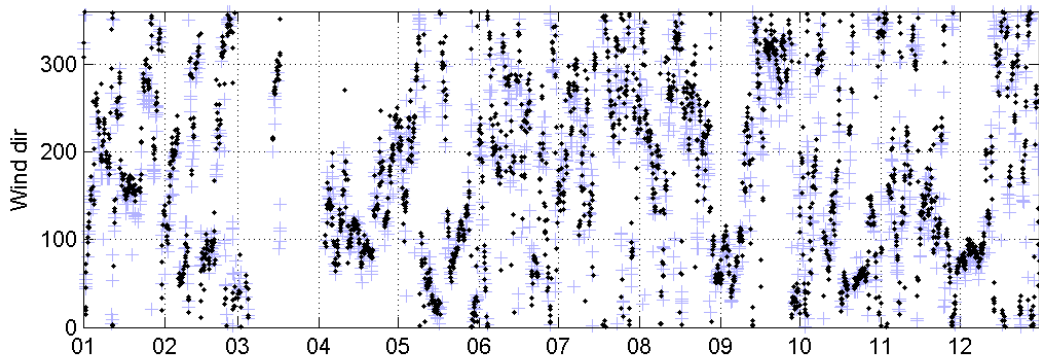
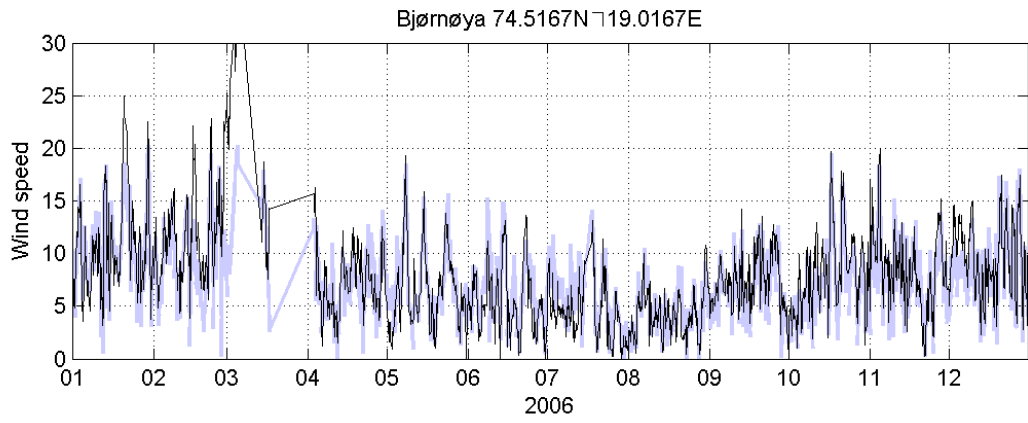
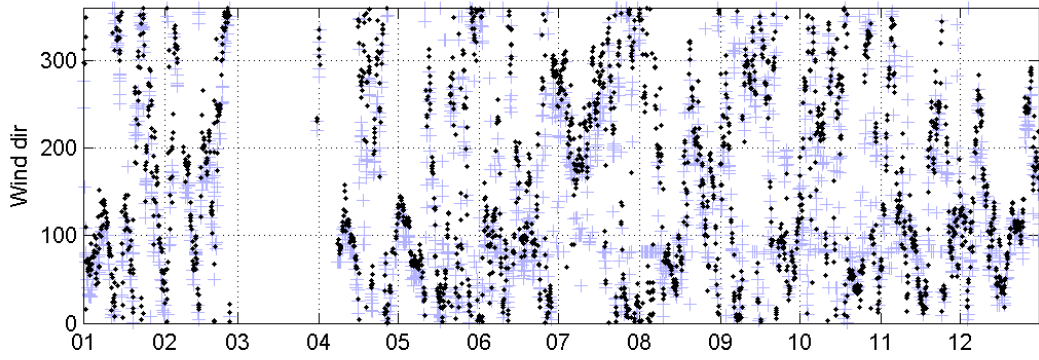
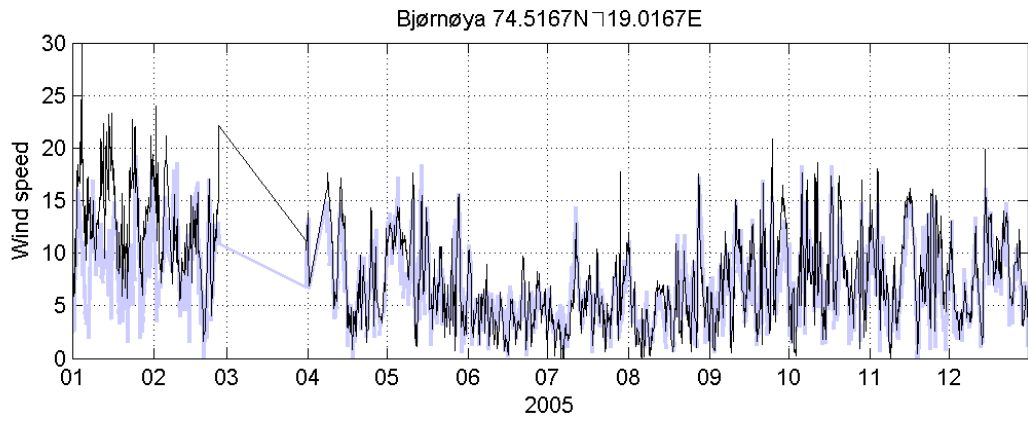


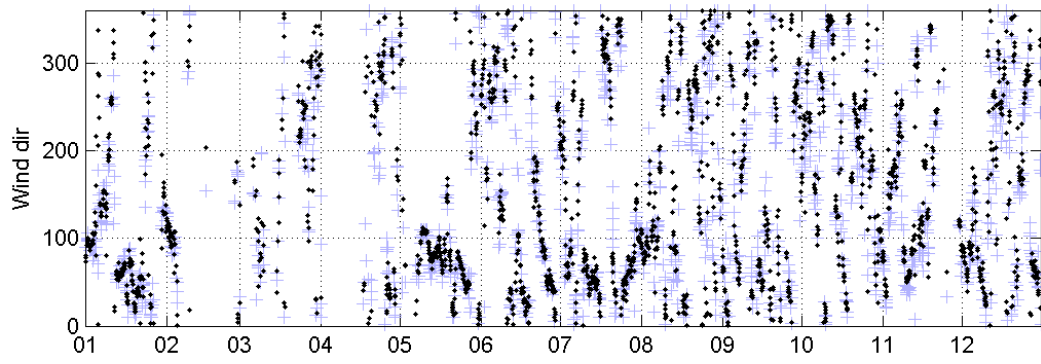
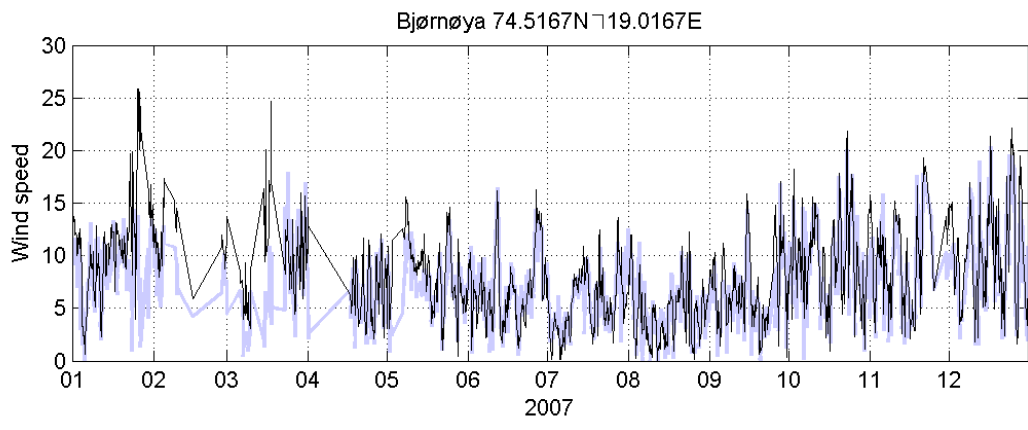
6.6 Bjørnøya



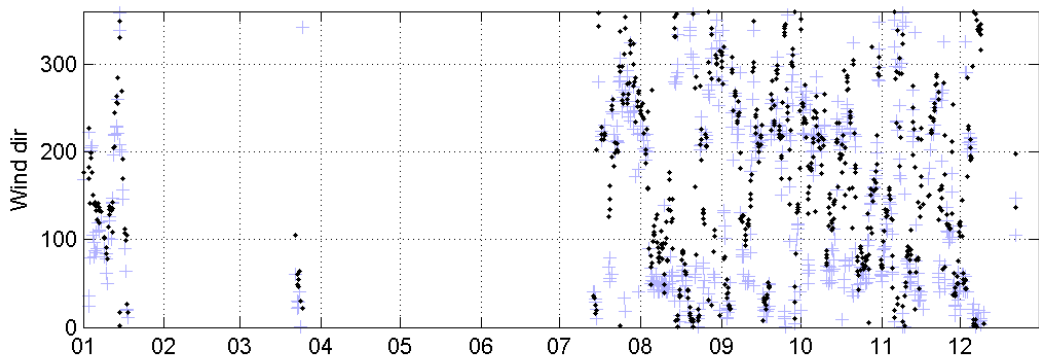
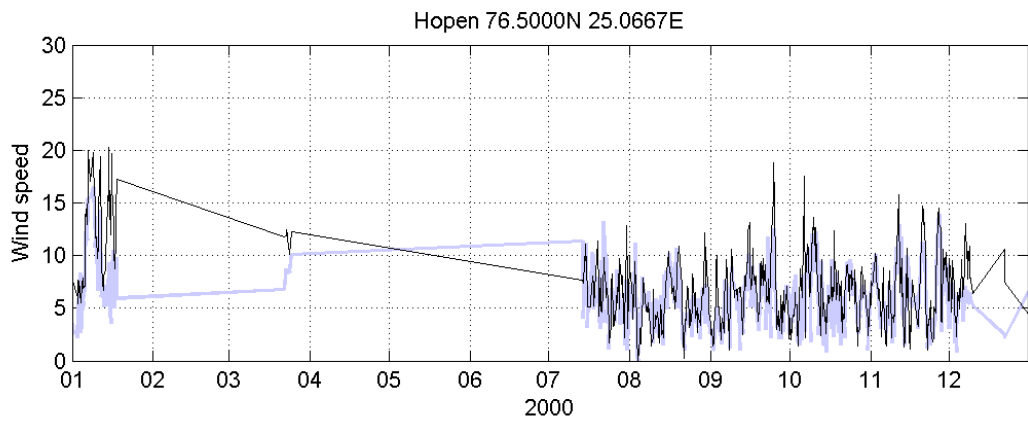
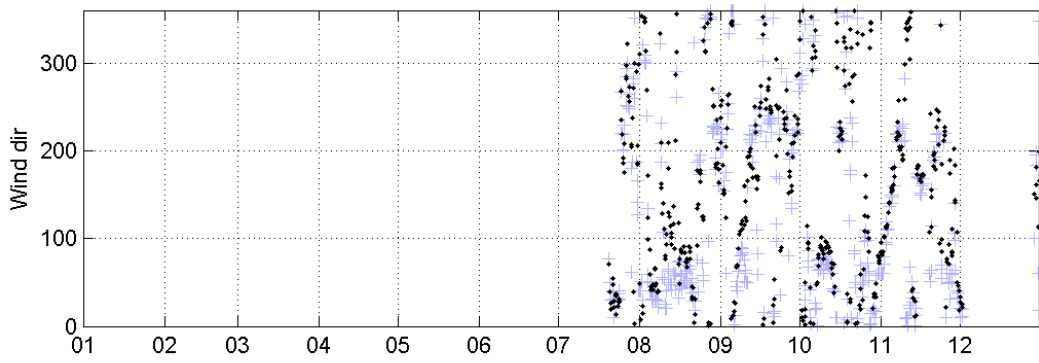
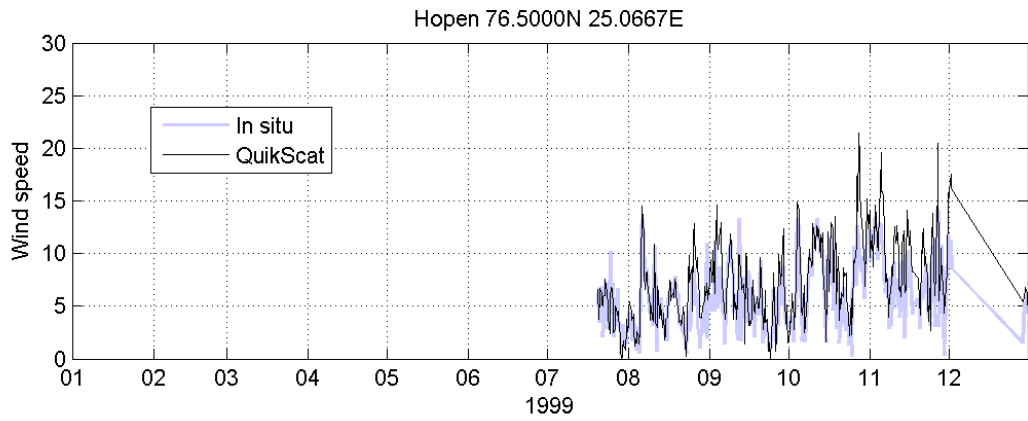


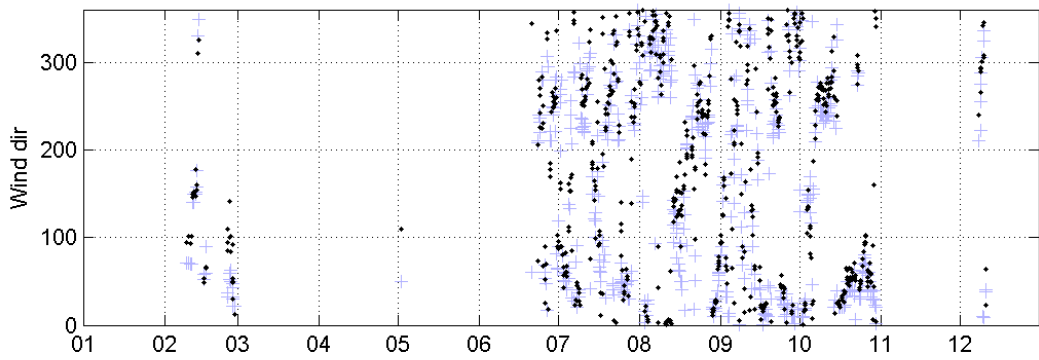
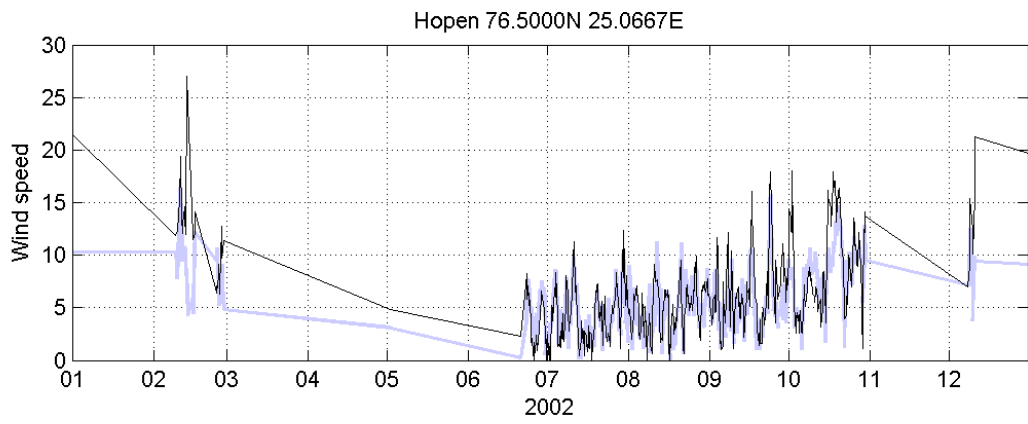
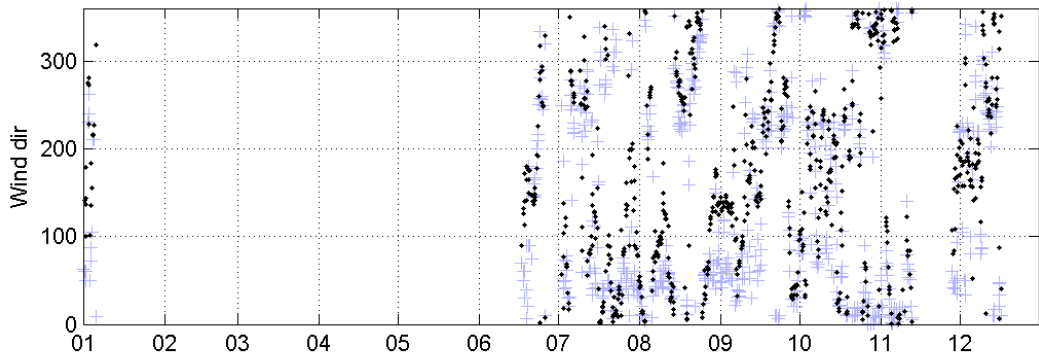
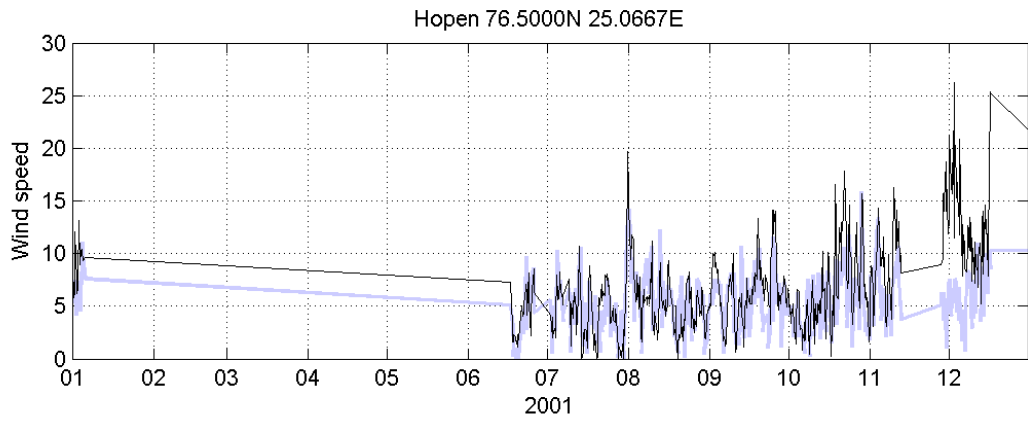


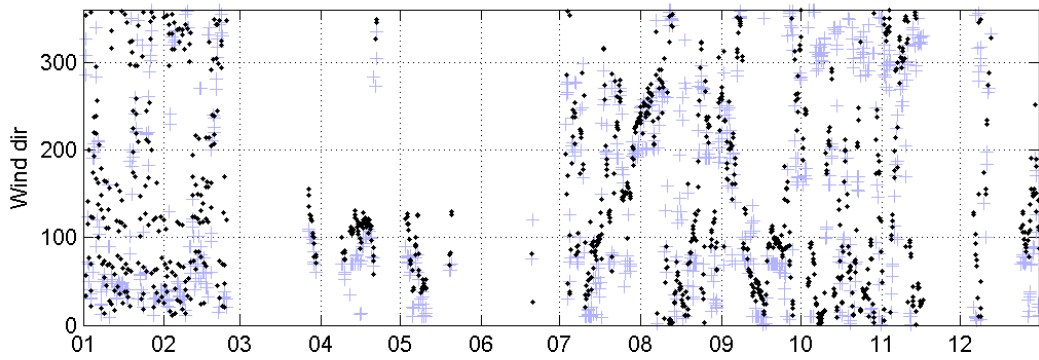
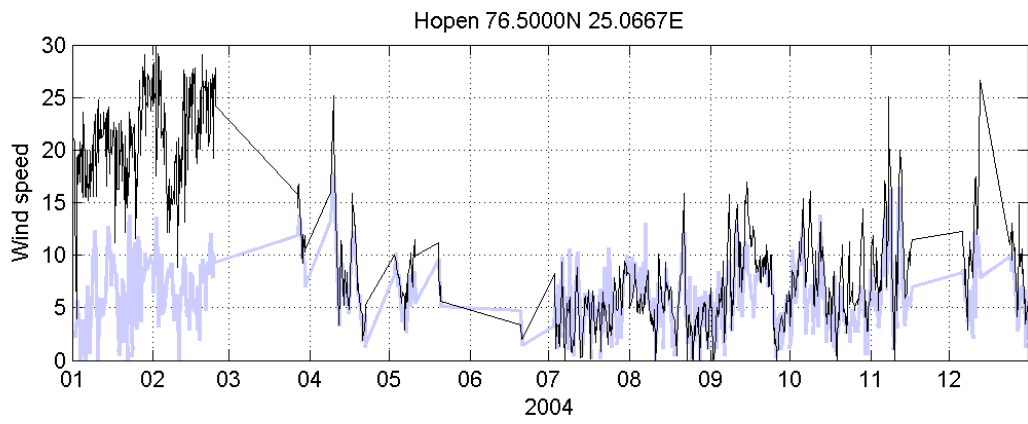
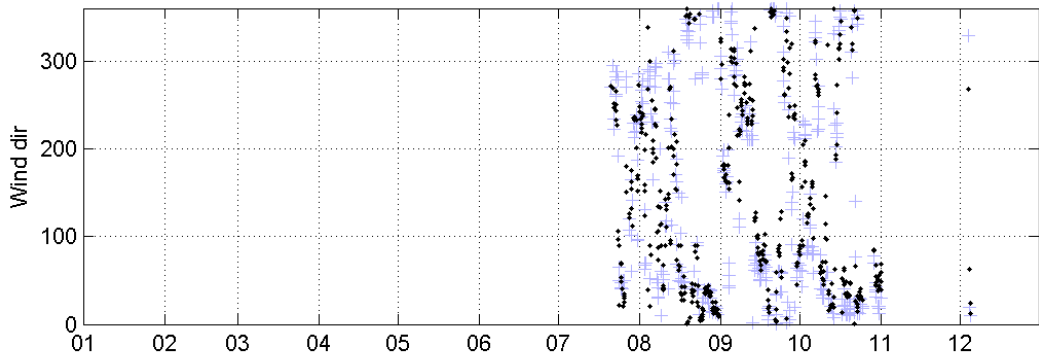
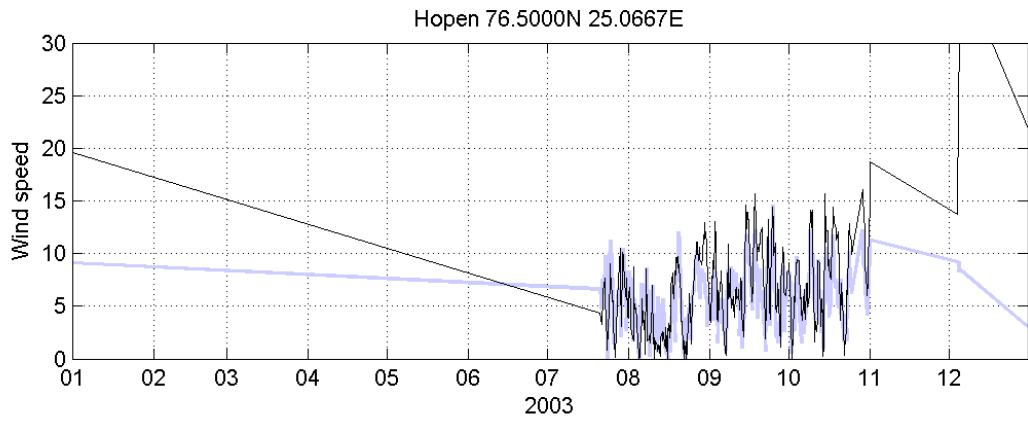


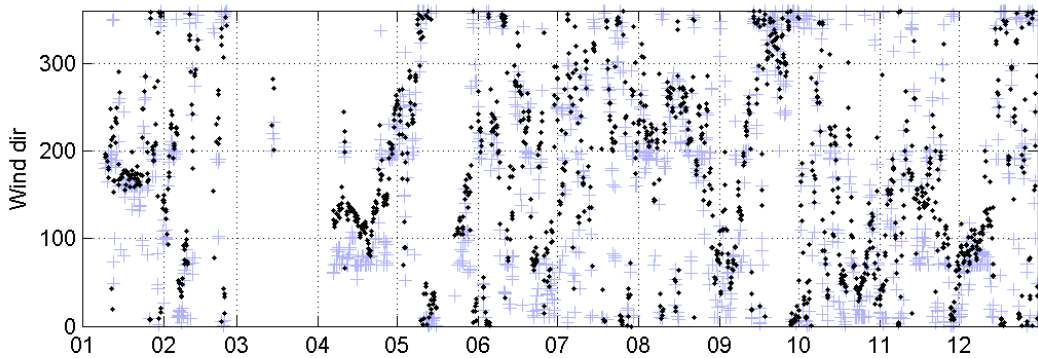
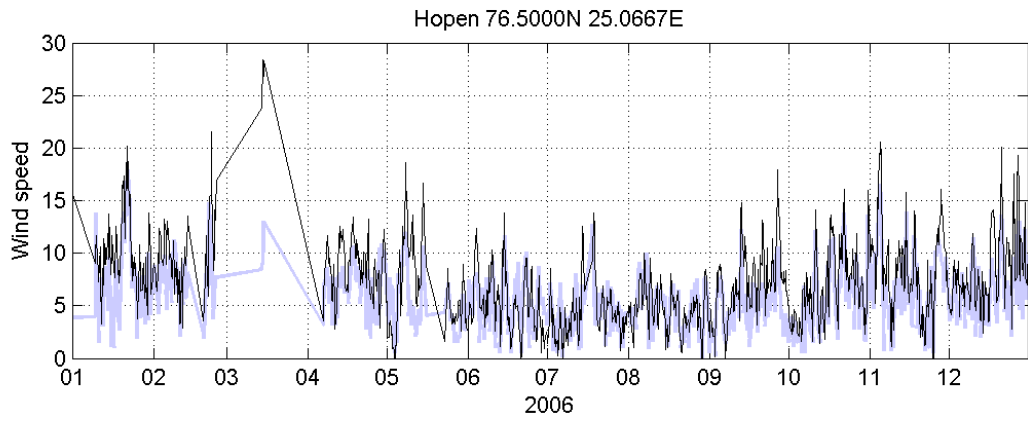
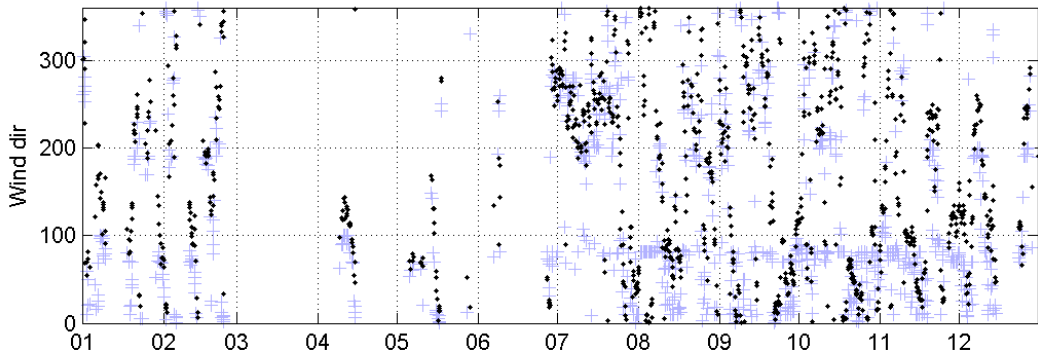
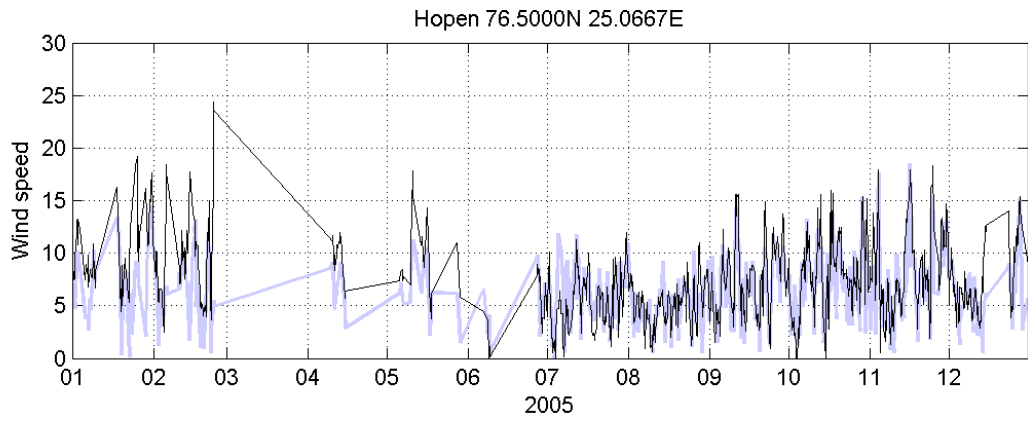


6.7 Hopen









Hopen 76.5000N 25.0667E

